COMPARISON OF 3D ROTATIONAL ANGIOGRAPHY WITH DIGITAL SUBTRACTION ANGIOGRAPHY IN SUB CLASSIFICATION AND TREATMENT PLANNING OF DIRECT CAROTID CAVERNOUS FISTULA

THESIS SUBMITTED IN PARTIAL FULFILLMENT FOR DEGREE OF

DM (NEUROIMAGING AND INTERVENTIONAL NEURORADIOLOGY (2015-2017)

OF THE SREE CHITRA TIRUNAL INSTITUTE FOR MEDICAL SCIENCES AND TECHNOLOGY

TRIVANDRUM, INDIA

Dr. SAVITH KUMAR

DEPARTMENT OF IMAGING SCIENCES & INTERVENTIONAL RADIOLOGY SREE CHITRA TIRUNAL INSTITUTE FOR MEDICAL SCIENCES AND TECHNOLOGY, TRIVANDRUM, INDIA

SREE CHITRA TIRUNAL INSTITUTE FOR MEDICAL SCIENCES
AND TECHNOLOGY, TRIVANDRUM

CERTIFICATE

This is to certify that the work incorporated in this thesis titled **"Comparison of 3D Rotational Angiography with Digital Subtraction Angiography in sub classification and Treatment planning of Direct Carotid Cavernous Fistula"** for the degree for DM (NEUROIMAGING AND INTERVENTIONAL NEURORADIOLOGY) has been carried out by Dr. Savith Kumar under our supervision and guidance. The work done in connection with this thesis has been carried out by the candidate himself and is genuine.

(Dr Santhosh Kumar K)
Associate Professor
Principal Guide

(Dr Jayadevan E.R)
Additional Professor
Co-Guide

Dr TR Kapilamoorthy
Professor & HOD
Department of Imaging Sciences and Interventional Radiology,
SCTIMST, Thiruvananthapuram.

DECLARATION

I hereby declare that this thesis titled **"Comparison of 3D Rotational Angiography with Digital Subtraction Angiography in subclassification and Treatment planning of Direct Carotid Cavernous Fistula."** has been prepared by me under the supervision and guidance of Dr.Santhosh K (Associate Professor), Dr Jayadevan ER (Additional Professor) and Dr.Kapilamoorthy TR (Professor & HOD), Department of Imaging Sciences and Interventional Radiology, Sree Chitra Institute for Medical Sciences and Technology, Trivandrum.

Date: (Dr Savith Kumar)

Place: Thiruvananthapuram

ACKNOWLEDGEMENT

- I am deeply indebted to my teachers and guides **Dr Santhosh K and Dr Jayadevan ER** for their constant unwavering support, insightful criticism, expert supervision and patience throughout this study.

- I am profoundly grateful to **Dr Kapilamoorthy TR, Dr Kesavadas C, Dr Bejoy Thomas** and for extending their guidance whenever needed.

- I would specially like to acknowledge my gratitude to my past and present colleagues and the technologists in the department for their valuable assistance at all times.

- I would also like to extend my heartfelt gratitude to my family for being immensely supportive and patient all through my endeavours. I could not have achieved a fraction of what I have without their prayers, love and support.

- Last but not least I am eternally grateful to all my patients & their relatives who have been very understanding and generous with their cooperation all through the study.

Dr. Savith Kumar
Senior Resident,
Dept of IS & IR,
SCTISMT,
Thiruvananthapuram,
India

CONTENTS

Introduction

Carotid-cavernous fistulas (CCF) is abnormal communications between the intracranial internal carotid artery (ICA) and or external carotid artery (ECA) with the cavernous sinus (CS). The connection may be direct, or indirect through the dural branches, based on which Barrow has classified them into four types. Direct CCF is a high flow fistula and based on the etiology; it can be classified as traumatic or spontaneous.

Treatment is imperative in direct CCF as they rarely resolve spontaneously and are associated with progressive visual symptoms and visual loss. The treatment has evolved from the first case treated by CCA ligation by Travers in the year 1809 to surgical ligation or trapping of the fistula to a new era of endovascular therapy (1). Currently, the mainstay of treatment is the endovascular approach, and the available options include embolization using balloons or coils, sealing of the rent using covered stents or newly introduced flow diverters (2,3). The endovascular procedure has a high success rate of 88% to 98% (4–6) with no to low complication rate (4–7) varying with the technique and the institution. Parent vessel occlusion (PAO) is an alternative option done in difficult cases, either endovascularly or surgically (2). Treatment failure and recurrence are noted in direct CCF with recurrence rate varying between 10 – 15 %. It is more common with the use of a balloon and is attributed to premature balloon deflation, rupture or migration (2,6,8). Recurrence is also seen with the use of other devices like coils(9), stents (10,11) and following parent artery occlusion. Technical failure rate up to 28% has been reported with the initial use of balloon (12).

The choice of embolic agent or hardware is depended on angiographic factors such as the size of the rent, degree of the shunt, operator preference and institutional experience. Sub-classification of CCF has been proposed based on the degree of the shunt, and this has been shown to be helpful in the choice of embolic agent (7). The pretreatment planning is usually

performed on 2D Digital subtraction angiography (DSA). Though Hubers and Mehriger-Heshimer manoeuver assist in localizing the site and size of rent, due to high shunt flow, the precise location is commonly obscured in most of the cases on biplane imaging. The advance in the technology has seen the advent of newer imaging algorithm like 3D rotational angiography (RA) and DynaCT. 3D RA has an excellent resolution and provides a true 3D view from various angles, thus improving the understanding of vascular morphology. The utility of 3D RA in pretreatment planning of intracranial aneurysms have been proven (13), Ishihara S et al. 2000, (14). There is no study accessing the utility of 3D RA in pretreatment planning of direct CCF or describing its angioarchitecture. The prior attempt to subclassify direct CCF was based on biplane images.

We intended to study the effect of the addition of 3D RA in treatment planning and selection of hardware in direct CCF and also attempt to subclassify the shunt objectively. We will also evaluate the angioarchitecture of the CCF on 3D DSA and compare the findings of 2D DSA with that of 3D DSA.

Aims and Objective

- Evaluating the effect of the addition of 3D rotational angiography in subclassification, treatment planning and selection of hardware.

- Describe angioarchitecture of direct carotid cavernous fistula on 3D rotational angiography.

Review of Literature

3.1 Introduction:

CCF is abnormal communication between the carotid arterial system and the cavernous sinus. They have been classified based on the etiology, flow dynamics, anatomy and arterial supply (2). Direct CCF is high flow fistulas and account for 80% of all CCFs (2). Trauma is the most common etiology for direct CCF. Indirect CCF is low flow fistula with indirect communication between one or many dural branches of ICA and/or ECA with the cavernous sinus.

The pathophysiology in CCF is mainly due to increased pressure in the cavernous sinus caused due to its arterialization (2). The triad of symptoms in direct CCF includes pulsatile exophthalmos, orbital bruit, and conjunctival injection (4). The symptoms are determined by the pattern of venous drainage: ocular and orbital symptoms are seen with anterior drainage, tinnitus with posterior drainage and very rarely intracranial hemorrhage or raised intracerebral pressure with cortical venous reflex (15).

DSA is the gold standard and is essential for the confirmation of the diagnosis and therapeutic planning. Other modalities like ocular Doppler, Computed Tomography Angiography (CTA) and Magnetic resonance Angiography (MRA) have found utility in the initial evaluation. The treatment has evolved from the initial direct surgical repaired performed by Parkinson in 1973 to endovascular management now. The endovascular management has evolved from detachable balloons (DB), described initially by Serbinenko to a wide array of options such as coils, stents and flow diverters (FD) available now(3,4,16)

3.2 History of evolution of treatment:

Benjamin Travers did the first documented surgical treatment for CCF in the year 1809 who ligated the common carotid artery in a patient presenting with pulsatile unilateral

exophthalmos. Carotid artery ligation became the treatment of choice over the next century; however, required refinement due to high morbidity and mortality (1,17). Professor Gioppi first recommended digital compression in 1856. Pulsatile exophthalmos was treated by orbital vein ligation by Lansdown in 1874. Francis W. Murray first attempted ICA ligation as a treatment in 1904. Locke's in his autopsy studies showed that in traumatic CCF there is a direct fistulous connection between ICA and CS. Walter Dandy first reported intracranial ICA clipping for treatment of CCF in 1939. Hamby adopted intracranial suturing of the supraclinoid ICA as a treatment in 1964. Hamby and Gardner used flow directed muscle embolus introduced through the cervical carotid artery for occlusion of the fistula after carotid ligation.

In 1971 Parlo & Hanberry occluded the CCF using a nondetachable balloon which involved the sacrifice of the ICA. This was the beginning of a modern era or endovascular surgery. Parkinson first performed direct surgical approach with preservation of the parent artery in 1973. Serbinenko in 1974 was the first to treat CCF with DB with preservation of the parent artery. This unleashed the new era of endovascular management. In 1974 Mullan performed intracranial wire and gelatine sponge thrombosis of CCF via surgical transvenous route (17). Till 2003, DB was widely used as it was a relatively inexpensive and simple option. Since 2003 this device has been withdrawn from the US market due to the problem in balloon valve mechanism; however, it is still available in rest of the world (18). Currently, the mainstay of treatment is transarterial or transvenous endovascular embolization of the CCF with coils or liquid embolic agents (19). The other available options are covered stents and flow diverters (3,16,19). Some centers continue to use DB as it is relatively inexpensive and simple to use.

3.3 Aetiology and classification:

The CCF has been classified based on the etiology (traumatic, spontaneous or iatrogenic), flow dynamics (high flow or slow flow), anatomy (direct or indirect) and arterial supply (ICA, ECA or both). The most widely used classification based on angioarchitecture was proposed by Barrow et al. which classified CCF into four types, i.e., type A to D. Barrow type A fistulas are high flow fistula with direct communication between the cavernous segment of the ICA and cavernous sinus caused due to traumatic laceration of arterial wall or rupture of the cavernous ICA aneurysm; with trauma being commonest etiology. Spontaneous CCF is caused by rupture of cavernous ICA aneurysm or a weakened atherosclerotic arterial wall. Connective tissue disorders like Ehlers-Danlos syndrome, fibromuscular dysplasia, and pseudoxanthoma elasticum predispose to the development of spontaneous CCF (2).

Direct CCF is high flow fistulas and account for 80% of all CCFs (2). The other types (B to D) are low-flow fistula with indirect communication between one or many dural branches of ICA and/or ECA with the cavernous sinus. Direct CCFs usually arise after trauma or a ruptured aneurysm. Traumatic fistulas usually occur in young men and are seen in 0.2-0.3 % of craniofacial trauma (20). CCF may be caused by blunt trauma or penetrating head injury. CCF is a rare and unique complication associated with oblique and transverse central skull base fracture (21). The overall incidence of CCF in skull base fractures is 3.8% with the incidence of anterior, middle and posterior fossa fractures being 2.4%, 8.3%, and 1.7%, respectively(12). Skull base fracture is seen in up to 32 % of the traumatic CCF (12). In traumatic CCF the rupture of the artery could be due to tearing of the artery by the bone fragment, the shearing force acting on the vessel wall or due to increased intraluminal pressure from distal compression of the vessel (22). Traumatic CCF can rarely be bilateral

seen in 1-2% of the cases and is associated with a severe head injury which is fatal and thus are usually infrequent (2).

Direct CCF's due to ruptured aneurysms occur most frequently in middle-aged and elderly women (20). About 2-9% of intra-cavernous carotid aneurysms are complicated by a direct CCF (20). Unilateral CCF can present with bilateral or contralateral orbital symptoms which depends on the venous drainage through the intercavernous sinus. Approximately 20% of direct CCFs are not related to a history of trauma and regarded as spontaneous (23). Iatrogenic causes for direct CCF include transsphenoidal surgery, endovascular procedures, and percutaneous trigeminal rhizotomy (2,24).

The traumatic CCF has been subclassified based on the size into small, medium and large size fistula. This is determined by the presence of antegrade flow in the anterior cerebral artery (ACA) and/ or middle cerebral artery (MCA)(7). Small fistula on angiogram show antegrade flow in both ACA and MCA, medium-sized fistula in either MCA or ACA and large fistula show complete steal across the fistula with no antegrade flow. A Large fistula is seen in 5% of the cases, and if these patients do not have contralateral neurological deficit tend to have good willisian collateral (2). The subclassification is helpful in choosing the best endovascular treatment option (7).

3.4 Pathophysiology and symptoms:

The direct fistula allows the flow of pressurized arterial blood into the cavernous sinus leading to an increased surge of the pressure in the cavernous sinus. The resultant venous hypertension leads to dilatation of the cavernous sinus and arterialized flow in the draining veins. This revised venous drainage of the cavernous sinus and venous hypertension is responsible for most of the symptoms. Most often the revised venous drainage is multidirectional (24,25). The signs and symptoms depend on the adequacy and direction of drainage pathway, the size, and location of rent and presence of arterial collaterals. (2,24).

The classic presentation of direct CCF is the Dandy's triad of sudden onset exophthalmos, cephalic bruit, and conjunctival congestion. Complete clinical triad is not always found as the combination of the symptoms is dependent on the direction of the venous drainage and the size of the defect. Symptoms are often abrupt in onset and rapidly progressive. The symptoms can be classified as ocular, orbital, cavernous and intracranial with ocular/orbital symptoms being most common.

The clinical presentations included orbital bruit (80 - 98%), proptosis (72 - 81%), chemosis (55-78%), cranial nerve palsy (43-55%), conjunctival injection (44 - 55%) and visual impairment (26-39%) (5,7,20). Increased pressure in the orbital veins leads to orbital venous congestion and transudation of interstitial fluid into the orbit with resultant proptosis, conjunctival congestion, chemosis and periorbital edema. Increased intraocular pressure (IOP) is a result of impaired drainage of aqueous humor caused due to increase in venous pressure and secondary open angle glaucoma. The rapid development of choroidal effusion and obstructed lateral drainage of the globe by anterior displacement of iris due to raised IOP is known to cause angle-closure glaucoma (26). Neovascularization of iris secondary to retinal ischemia is also known to cause glaucoma**.** Rupture of subconjunctival vein leads subconjunctival hemorrhage. Corneal damage is caused by exposure keratitis (2,24,25). The

choroidal and retinal changes include choroidal effusion, retinal venous dilatation, central retinal vein occlusion, central retinal artery occlusion, cotton wool patches and serous retinal detachment(27,28). The visual impairment to some degree is seen in 60 -90% of the cases with 25% showing a total visual loss (4,29,30). Visual impairment may be secondary to corneal, retinal or optic nerve changes (27). Diminished vision is also caused by impaired retinal perfusion secondary to elevated IOP (2,24,25).

The causes for visual loss may be reversible and irreversible all of which are due to a cascade of changes caused by venous congestion and elevated IOP. Most of the reversible changes become irreversible if they are long-standing. Knowledge of the various causes is essential in choosing patients and when explaining the prognosis to the patient. The reversible causes of total visual loss include retinal ischemia, optic neuropathy caused by mechanical axonal conduction block secondary to elevated IOP and external compression on optic nerve by enlarged cavernous sinus and SOV or optic nerve ischemia, opacification of the cornea and lens due to edema and opacification of the media due to virtual hemorrhage. Irreversible causes for total visual loss are direct optic nerve injury during initial trauma, optic infarction and atrophy, neovascularization of iris and retina due to chronic ischemia, superior ophthalmic vein (SOV) thrombosis with associated retinopathy and choroidal effusion, retinal detachment, hemorrhage and retinal infraction (29,30).

Cavernous symptoms include diplopia and ptosis caused by cranial nerve dysfunction secondary to compression caused by increased venous pressure in the cavernous sinus. There may be isolated involvement of the 3^{rd}, 4^{th} and 6^{th} cranial nerves or in combination. Abducent nerve is more commonly involved in 49% of the cases with less common involvement of the 3^{rd} and 4^{th} nerve. Involvement of the 5^{th} cranial nerve usually the ophthalmic division is also seen (5,20,24). Diplopia can also be due restricted ocular movement caused by proptosis and edema of the extraocular muscles. Tinnitus is caused due to posterior venous drainage.

Intracranial symptoms include TIA and strokes caused due to steal phenomenon. Intracranial hemorrhage is seen in 3 to 5% of cases, caused by cerebral cortical venous hypertension which is a result of revised venous drainage into the sphenoparietal sinus, superficial middle cerebral vein or deep veins and occlusion of other drainage pathways (24,25,31,32). Brain stem edema has also been reported, which is caused due to venous congestion and increased drainage pressure in the brain stem veins(33). The rarer presentations of traumatic CCF are epistaxis and otorrhagia, seen in 0.8 to 3% of cases (31,34). Clinical symptoms of direct and indirect CCF overlap but there is difference in the onset of symptom and severity. Direct fistulas rarely resolve and require immediate treatment if there is a progressive visual loss, an intraocular pressure higher than 40 mm Hg, rapidly progressive proptosis, corneal exposure, intolerable bruit, severe retro-orbital pain, increased intracranial pressure, intracranial hemorrhage, and TIA(24,31,35). The angiographic features which warrant an immediate treatment are cortical venous reflux, pseudoaneurysm, and cavernous sinus varix (Table 1). The goal of treatment is to eliminate the fistula with preservation of the patency of the ICA (20,31).

Angiographic indicators for emergency treatment (24,31)

Angiographic Feature	Risk
Pseudoaneurysm	Rupture
Venous aneurysms or Varix	Thrombosis and hemorrhage
Cortical venous reflex	Intracranial hemorrhage and edema
Distal outflow pathway thrombosis	Intracranial hemorrhage and edema

Clinical indicators for emergency treatment

Clinical features	Risk
Progressive visual loss	Irreversible visual loss
Corneal exposure	Corneal opacity (irreversible damage)
Rapidly progressive proptosis	Visual loss and exposure keratopathy
Intolerable bruit	-
Severe retro-bulbar pain	-
Raised ICP or ICH	-
TIA	-
Epistaxis and Otorrhagia	Catastrophic haemorrhage

Table 1: Angiographic and Clinical Indicators for Emergency Treatment

The diagnosis of traumatic CCF is relatively straightforward in an appropriate clinical setting of trauma with typical symptoms of pulsatile proptosis, cephalic bruit, and conjunctival congestion. The pretreatment evaluation includes: detailed eye evaluation to document the visual acuity, visual field, IOP, and fundoscopy.

3.4 Imaging:

Non-invasive imaging (CT, MR, and Doppler) is often used in the initial workup of a possible CCF. The findings of proptosis, thickening of the extraocular muscles, retroocular fat stranding, dilated and tortuous SOV, and bulging of the cavernous sinus are seen both on CT and MRI (22). CT is superior in the evaluation of the skull base fractures, and MRI better demonstrates the orbital and brain parenchymal changes. In patients with cerebral venous congestion and raised intracranial tension, cerebral edema and hemorrhage are also encountered. CTA and MRA have also been used for initial evaluation of a patient with direct CCF. CTA is demonstrated to be as useful as DSA in the initial detection of the direct CCF and the identification of the size and location of the rent and performed better than MRA(36). Direct CCF is detected by identifying the dehiscent ICA on multidetector CT and also they provided anatomical detail of the fistula like the size, location, direction and the venous pouch size (37).

Doppler performed through orbital, temporal and occipital windows has value in diagnosis and follow-up of CCF, and it is complementary to angiography. Doppler findings described include the direct sign of irregular color mosaic in the enlarged cavernous sinus, hemodynamic changes like the lower resistive index in the ipsilateral ICA and lower peak systolic velocity distal to the fistula compared to the healthy side and reversed pulsatile arterial flow in SOV(38,39).

DSA is the gold standard for evaluation of CCF. It is essential for diagnosis, classification, and planning intervention. It best characterizes the size and location of the fistula, venous drainage pattern and cortical venous reflex. It is useful to assess the associated vascular injuries like dissection and pseudoaneurysm, cerebral circulation and steal phenomenon. DSA also provides information on the collateral flow, circulation time and venous delay which is essential for planning treatment. Detection of the site of rent is

challenging on DSA because most direct CCFs are high-flow fistulae, causing flow related washout of the intra-arterial contrast and the cavernous sinus is usually immediately opacified on angiography, thus obscuring the precise communication site. Particular maneuver to reduce the flow rate have been tried which includes Mehringer-Hieshima maneuver, Heuber, and double-lumen balloon catheter. Mehringer-Hieshima maneuver consists of a selective angiogram of ipsilateral ICA obtained at slow frame rate with simultaneous digital compression of the ipsilateral common carotid artery (40). The Heuber maneuver consists of a selective angiogram of the dominant vertebral artery obtained with simultaneous digital compressing the ipsilateral carotid artery (41,42). Double-lumen balloon catheter technique involves selective angiogram obtained through the dual lumen balloon microcatheter catheter after inflation of the balloon in the petrous ICA (43).

Before any treatment is planned tolerance of cerebral hemisphere to ipsilateral ICA occlusion need to be tested. The gold standard is performing the balloon occlusion test (BOT). BOT is done by temporarily occluding the ICA and doing a clinical surveillance to look for signs or features of hypoperfusion. This is also combined with an adjunctive assessment like hypotension challenge, stump pressure measurement or transcranial doppler(44).

The precise communication site in direct CCF may remain obscured on biplane DSA even after the use of specific maneuvers. Though DSA is the standard imaging procedure for endovascular treatment, with an excellent spatial and temporal resolution, it cannot give an accurate three-dimensional view from every angle.

The 3D RA images have excellent resolution and can be rotated in any direction to show the structures from any required angle, including views that would be impossible to obtain by radiographic projections alone. An improved understanding of the 3D vascular morphology helps to ensure optimum positioning of the C-arm during the intervention for

positioning of the catheters, coils, balloons, and stents(45) and for the planning surgery which has been proven in case of intracranial aneurysms(13,46). Studies in intracranial aneurysms have also show 3D to be better in depicting the size of an aneurysm and picking up recurrent/residual aneurysms on follow up(47,48). 3D RA has also been used in planning treatment and assessing the adequacy of embolization in direct CCF; however, these studied are confined to case reports(49,50). 3D RA in these reports best demonstrated the relationship between the ICA, fistula and the cavernous sinus sac(50).

3.5 Treatment:

Different series have proposed different strategies according to the physician experience and preference in addition to the characteristics of traumatic CCF such as type, size, location, and availability of the modalities.

3.5.1 *Endovascular: Transarterial and transvenous*

Endovascular management is the mainstay of treatment with a number of options available. Detachable balloons, coils, liquid embolic agents (LEA) and stents have all been used. Each of the devices has their advantages and disadvantages. The approach and the choice of device differ from cases to case and is chosen based on the specific anatomy and the operator preference. The characterization of the location and dimension of the fistula is essential to select the best treatment option. The goal of endovascular treatment is to interrupt the abnormal communication but preserving the patency of the parent artery. This can be achieved by obliteration of the fistula with a detachable balloon, occlusion of the cavernous sinus with coils and/or LEA or deployment of the stent across the rent (18). Interruption of the fistula ensures a reduction in the cavernous sinus venous pressure, in turn reducing the compression on the cranial nerves, orbital and ocular venous congestion and also improve

cerebral perfusion (25). When the defect is large or there is arterial transection which cannot be repaired, then artery has to be sacrificed. The transarterial approach is superior due to the easy navigability of the microcatheter into the cavernous sinus as there is high flow across the defect(25). The transvenous approach is chosen in the case of recurrence where the transarterial access is not possible or difficult.

Balloon: Serbinenko developed the first DB with the indigenous valve mechanism. Debrun et al. developed latex tie on DB in 1974. Later Latex and Silicon balloon with internal valve and various modifications were developed (Table 2).

Detachable Balloon	Manufacturer
Detachable Silicone Balloon	Target Therapeutics Corporation
Debrun Tie-on Latex Balloon	Nycomed, Paris, France
Gold Valve Latex Balloon	Nycomed, Paris, France
Latex String Valve and Integral Valve	Balt, Montmorency, France
GoldBal Latex Balloon	Balt, Montmorency, France

Table 2: Detachable Balloons(42)

	Latex Balloon	Silicon Balloon
Dispensability	Greater	Lesser
Coefficient of Elasticity	8	4
Thrombogenicity	More	Less
Endothelialisation	Rapid	Delayed
Semipermeable	No	Yes
Cost	Less expensive	Costlier
Duration Inflation	3 – 5 weeks	Months

Table 3: Differences between Latex and Silicon Balloon(42).

The advantages and disadvantages of the latex and silicone balloon are illustrated above (Table 2). The Latex balloons are thrombogenic due to its surface texture and local tissue reaction. Because of the high elasticity latex balloon are more durable when inflated to the same degree as silicon balloon. The osmolality of contrast used for inflation of Latex balloon is not crucial as Silicon balloon as they are not semipermeable like silicon balloons(42). The Tie-on Latex balloons are delivered using a Coaxial Teflon Catheter. Goldbal latex balloons are the once which are available now; they have an internal valve and a radiopaque metal marker. They are deployed either by gentle traction using single microcatheter [MAGIC or BALTACCI microcatheter for Detachable Balloon with a PolyEthylene distal part (MABDPE or BALTACCIBDPE)] or by pushing the outer catheter using coaxial system (COAX). The balloon is inflated with hypertonic water-soluble contrast material (1:1 dilution). Rapid deflation of the balloon leads to recurrence or formation of pseudoaneurysms.

The balloon should remain inflated for at least one week for development of fibrous attachment with the vessel wall and permeant occlusion of fistula. Post-procedure care includes complete bed rest, in particular, restricted head movement for 24 hours(8). Transarterial DB has been the widely preferred option because for the procedural simplicity, cost-effectiveness and safety.

The DB has been withdrawn from the market in the United States of America since 2003 due to problems related to the valve; however, it is available in rest of the world. The reported success rate of DB in excluding the fistula with preservation of the parent artery is 75% to 88%(4,5,20). The rate of parent artery sacrifice is 12.1%, the recurrence rate is 12 %, (8) and the failure rate is 5 - 10% (15).

Coil: Due to the non-availability of DB and it higher associated incidence of treatment failure and recurrence, detachable coils have become the mainstay of endovascular embolization.
When using detachable coils tight packing of the cavernous sac is required to achieve the complete sensation of the shunt. This is a problem in the case with large sac as large coil mass may lead to cranial nerve dysfunction and also increases the cost of the procedure. In difficult cases when dense packing is not possible its leads to recurrence. In cases with large rents there is always a risk of coil prolapse (25).

LEA: Onyx (eV3 Covidien, Irvine, CA, USA) as the only embolic agent has been tried with balloon used for protection. The drawback of this technique is prolonged balloon inflation which may lead to TIA when willisian collaterals are not adequate. There is also the risk of percolation of the agent into the small veins normally draining into the cavernous sinus (51,52)

Coil plus LEA: Onyx in association with the coils can be used when large numbers of coils are required to obliterate the fistula. Onyx is cheaper and allows for good reconstruction of the arterial tear and coils form scaffolding and retain the onyx by reducing the flow and thus allow for injection of the onyx without migration. This avoids dense packing of the cavernous sinus and thus preventing the cranial nerve palsy by coil mass compression(35). N-butyl-2-cyanoacrylate has also been used after partial coiling of the sac to occlude the fistula. It is essential to preserve the normal venous drainage of the Sylvain and ophthalmic vein. Balloon protection can also be used both during coil deployment and onyx injection. The incidence of the pseudoaneurysm formation is lesser with this technique (25,35).

Covered Stent: When the primary treatment options like the DB and the coils have failed or are not suitable in a complex fistula, the covered stent could be considered, particularly when the collateral circulation is inadequate(10). The currently available stents are Jostent coronary stent graft (Abbott Vascular, Redwood City, Calif), which is off-label and Willis covered stent (MicroPort, Shanghai, China) which is specifically designed for a pseudoaneurysm and intracranial aneurysm. Jostent is composed of the superposition of 2 stainless steel stents and an ultrathin polytetrafluoroethylene (PTFE) layer between them. Willis covered stent is a balloon-expandable bare stent and PTFE membrane. The reported complete occlusion rate with preservation of the parent artery is 83.3 - 92.6%. The rate of endoleak is < 50% which is always seen immediately(53,54). Drawbacks are a requirement of long-term antiplatelet therapy and rigid configuration which does not allow for easy navigability and may cause vasospasm. The antiplatelet therapy during the pre-operative period may hinder in the thrombus formation around the fistula. The complications are intraprocedural and post-procedural thromboembolism, endoleak and in stent stenosis (53,54).

Flow diverter: Currently the trend in endovascular management is to move away from the deconstructive treatment towards reconstructive treatment. This is also applicable for CCF with large rent or transection of the artery. Flow diverters can thus be used as an adjunct to the coils or balloons for endoluminal reconstruction of the ICA in such cases. This facilitates endothelialisation of the ICA and presumably minimises the recurrence and other complications like pseudoaneurysm(16). Flow diverters have also been used solely with telescoping of multiple devices to achieve higher metal surface coverage at the fistulas site. The drawbacks are cost, and of long-term antiplatelets use (3). In the past seven years since the first treatment 23 cases have been reported with a total success rate of 100%(16).

Transarterial approach with balloon protection of the parent artery: Coil and onyx under intra-arterial balloon protection: The procedure is performed by using a compliant balloon for protection of the artery and navigating the microcatheter super selectively into the cavernous sac across the rent. Detachable coil embolization is performed at the main site of the fistula and near the draining venous outlet to achieve partial embolization of the sac and provide a framework for subsequent onyx embolization. Dense coil packing is not necessary. Balloon protection is used to prevent coil prolapse. Subsequently, the onyx is injected into the sac with inflated balloon occluding the fistula. The onyx is injected into the coil mass which traps the LEA and prevents the cast from entering into the normal draining veins. Total angiographic obliteration is the preferred endpoint(52). The advantages of precoiling with onyx embolization are; the coil and onyx form a reinforced structure which prevents migration of either of them on deflation of the balloon. The number of coils and volume of onyx required to achieve fistula obliteration is less. Thus the duration of ICA occlusion is less. Dense coil packing is not needed, thus reducing the chances of cranial nerve dysfunction and cost. Coil mass in the cavernous sinus slows down the flow preventing onyx from casting

freely and provides a scaffolding for cast formation (25). C.E. Baccin reported first embolization using coil and onyx with balloon in 2005(35). Ying Yu et al. found this technique to be an effective and safe option for treatment of CCF with a large defect and cavernous sac (25) with rare complications.

Transarterial approach with stent protection of the parent artery: Transarterial embolization of the venous sac can also be performed with the use of intracranial self-expanding stents for protection. They offer a similar advantage as balloons used for protection but with a drawback of requirement for long-term antiplatelet therapy.

Primary Transvenous approach: The cavernous sinus is accessed through the transvenous approach. A protection balloon is placed in the ICA across the fistula through the transarterial approach. Under balloon protection, the venous pouch close to the fistula is obliterated using coils. This approach is preferable for small fistulas as it allows for stable and selective coiling of the venous sac close to the fistula with lesser number of coils used unlike transarterial venous sac(55). The transvenous approach is also chosen when there is no transarterial access available as in recurrence after PAO occlusion of the ipsilateral carotid artery.

3.5.2 Endovascular: PAO

PAO is performed in difficult cases where reconstructive techniques are not feasible, like large rents, transection of the artery, cases associated with arterial dissection or recurrent cases.

3.5.3 Newer techniques:

The mainstay of treatment in direct CCF is transarterial embolization with coils and other embolic agents. New endovascular technologies like the newer devices and embolic agent have been developed to ease the procedure and also newer techniques have been tried to overcome some specific situations.

Dual lumen balloon technique: Samaniego EA et al. described the transarterial balloon-assisted embolization of the direct CCF with dual lumen balloon microcatheter Scepter C (Microvention, Tustin, California, USA). The double lumen balloon microcatheter served two purposes; one to characterize the arterial wall defect and second for protection of the ICA during embolization. Scepter C dual lumen balloon microcatheter is navigated into the petrous ICA and inflated to achieve flow arrest. Then an angiogram through the balloon catheter lumen is performed to assess the size and location of the fistula which determines the best endovascular treatment. If the rent is ≤ 3mm detachable coils and/or onyx (Covidien, Irvine, California, USA) is used. The embolization is performed through the balloon microcatheter after navigating the distal 5 cm tip of the device into the cavernous sinus through the defect with the parent vessel protected by the balloon portion of the device. In cases with rent is ≥ 4mm then stent-assisted coiling is performed. The advantage of this technique is both parent artery remodeling, and embolization can be performed with a same device and characterization of the carotid wall defect is possible, which the author found extremely useful in choosing the best treatment option (43).

Plug Device: Microvascular plug (Reverse Medical, Irvine, Calif., USA) is a new device available for treatment of direct CCF. This technique offers easy navigability through tortuous arteries and immediate occlusion(56).

Material and Methods

4.1 Study design:

This is a comparative study in a retrospective-prospective design, performed after obtaining appropriate clearance from our institutional ethical committee (letter no SCT/IEC/807/August-2015 dated 6 Feb 2016). The retrospective arm included the period from Jan 2010 to13 Aug 2015 and the prospective arm from 13 Aug 2015 till 31 May 2017. Subjects included consecutive patients with traumatic CCF who were treated in our institute from the period of 1 Jan 2010 to 31 May 2017.

4.2 Patient selection:

The prospective cohort was enrolled from Neurosurgery, Neurology or Radiology OPD, comprising of consecutive patients of traumatic CCF. The hospital electronic database was searched using search words of "traumatic carotid cavernous fistula", "Carotid cavernous fistula", "Type A Carotid cavernous fistula" and "caroticocavernous fistula" and all patients who had both 2D DSA and 3D RA images of good quality and were treated in our institute were enrolled into the retrospective arm of the study.

Inclusion criteria*:*

- All patients with traumatic CCF who underwent endovascular treatment from 1 Jan 2010 to 31 May 2017 irrespective of age, sex or ethnicity.
- Presence of both 2D DSA and 3D RA images of good quality.

Exclusion criteria:

- Patients in whom 3D RA was not performed.
- Patient in whose appropriate data was not available on PACS or electronic medical records.
- Patients with contraindication for the use of iodinated contrast.
- Patients or relatives who do not give consent for the study.

Patient details were anonymized and key generated to analyze the patient data.

4.3 Data Collection:

4.3.1 Clinical variables:

The demographic, clinical, radiological, interventional details and post-procedure outcome of the patients in the retrospective arm were obtained from the electronic medical records. These details of the patient in the prospective arm were obtained as and when the patient was admitted for intervention. The patient demographics details like age at presentation and sex, clinical symptoms and signs of proptosis, orbital congestion/chemosis, visual impairment, periorbital swelling, headache, orbital/retro-orbital pain, tinnitus, bruit, extraocular movement, ptosis, corneal reflex, facial sensation, visual field, visual acuity, IOP and funduscopic findings were recorded. The date of trauma, time duration from injury to first symptom & definitive management and time duration from first clinical symptom to definitive management were also recorded. IOP of more than 20 mm of Hg or a difference of more than 5 mm of Hg between two eyes were considered abnormal.

4.3.2 Cross-sectional Imaging:

The details of presence or absence of fracture (skull base, orbital and maxillofacial fracture), intracranial hemorrhage (intraparenchymal hematoma, subarachnoid hemorrhage, extradural hemorrhage and subdural hemorrhage) and parenchymal contusion were obtained. The skull base fractures were classified as anterior, central and posterior cranial fossa fractures. The central cranial fossa fractures were intern classified as central and transverse fractures (21).

4.3.3 Angiography:

All patients were imaged using a Biplane neuroangiographic unit (GE Innova 3131 Milwaukee USA) Image acquisition was performed using a dynamic flat-panel detector system with a 30 x 30 cm entrance plane, producing an image with a 1024 x1024 matrix**.** Iohexol 350 mg I/mL or Iodixanol 320 mg mL / I was used as contrast agent.

All angiograms were performed with the modified Seldinger method via femoral artery access. Standard 4-Fr or 5-Fr diagnostic catheters were used to perform the angiographic examination. In the first phase of the study, selective angiography of both CCA, ICA, ECA, and VA was performed in the AP, lateral, Towne's and oblique views (standard projections). Heuber and Mehringer-Hieshima manoeuvre was also performed. Following 2D DSA, 3D RA was performed on the vessel on the side of the fistula with a contrast injection of 20-25 ml (2:1 dilution) at a rate of 3 mL to 5 ml per second (delay of 1 - 2 sec). The contrast media was injected automatically using a pressure injector. 3D RA was acquired with following parameters: gantry rotation speed of 40°/s over 192°arc, field of view 30 × 30 cm, matrix size 512 × 512, acquisition time 5seconds, the total number of frames 147 and delay time 0–3 seconds. The reconstructed images were isotropic with a minimum thickness

of 0.3 mm. Acquired 3D images were processed on multimodality workstation (AW 3.1 GE Medical Systems).

The angiographic characteristics of the CCF on 2D DSA & 3D RA like the size, number and location of the fistula, size of the primary cavernous sac, presence or absence of antegrade flow in the ACA and MCA, venous drainage, cortical venous reflex, collateral circulation and circulation time were recorded.

4.4 Image Analysis:

The 2D DSA and 3D RA images were evaluated on GE advanced workstation by two independent reviewers (SK and SKK). 3D RA images were assessed by using the full range of post-processing parameters including multiplanar reformation. The 2D DSA images were evaluated first followed by combined evaluation of 2D DSA and 3D RA. The reviewers independently evaluated quantifiable (number, size, and location of rent, size of the primary cavernous sac and subclassification) and descriptive characteristics (quality of detection of number, size and location of the fistula and subclassification and was rated on a three-point scale). The therapeutic decision and the preferred embolic agent was determined by the readers independently based on 2D DSA alone, and combined 2D DSA and 3D RA and quality of this choice of response was also rated on the three-point scale.

4.4.1 Quantifiable characteristics:

The number, size, and location of the fistula and size of the adjacent cavernous sinus sac were analyzed. The number of rent was subcategorized into one, two and more than two. The size of the fistula was measured on one plane in 2D DSA and along two planes on 3D RA. When the precise measurement was not possible it was recorded as cannot be measured. The location of the rent was described with respect to the involvement of the five segments of

the cavernous ICA as classified by Debrun et al. (12) which included posterior vertical, posterior genu, horizontal, anterior genu and anterior vertical segments. Angiograms performed with Heuber and Mehringer-Hieshima manoeuvre were used to determine the quantifiable characteristics (size and location of rent) on 2D DSA by looking at the site of the first appearance of contrast outside the confines of the cavernous ICA. The wall of the ICA was well defined on 3D RA; the site of rent was determined by tracing the wall of the ICA to the site at which it became indistinct.

The traumatic CCF was subtyped as small, medium and large on 2D DSA depending on whether there was antegrade flow in ACA and/or MCA (7). Small fistula showed antegrade flow in both ACA and MCA, medium-sized fistula in either MCA or ACA and large fistula showed complete steal with no antegrade flow. The subtyping on 3D RA was performed based on the sector of involvement with $< 90^{o}$ being small, between 90^{o} to 180^{o} being medium and $> 180^{o}$ being large. The actual sector of defect in each case was also documented.

The two reviewers reached a consensus regarding the number, subclassification and location of the rent on 3D RA and their joint assessment was recorded. The findings were confirmed with the observations during embolization. This joint assessment was considered as a standard for comparison of the reading of the two reviewers.

4.4.2 Descriptive Characteristics:

The quality of detection of the number, size and location of the rent and subclassification based on 2D DSA alone and combine 2D and 3D RA were rated on the three-point scale as 1- good; 2- sufficient and 3- insufficient by each reviewer. Good was defined as accurately able to detect, sufficient as able to detect however not very confident and insufficient as not able to detect.

***4.4.3 Therapeutic decision*:**

The preferred treatment option and the preferred embolic agent based on 2D DSA alone and combine 2D and 3D RA was chosen by both the reviewers independently. The revivers had to choose whether the first treatment option is constructive or destructive. The constructive option included balloon or coil embolization of the venous sac or stenting across the site of fistula where the parent artery is preserved. Destructive option included PAO or trapping of the fistula. The preferred embolic agent for constructive treatment option was chosen between balloon, coil, stent and liquid embolic agent. The quality of this choice of response, i.e., the first treatment option and the preferred embolic agent was rated on the three-point scale 1- good; 2- sufficient and 3- insufficient by two reviewers independently. Good was defined as able to choose one option confidently, sufficient as able to choose one option but not with much confidence and insufficient as not able to choose one option.

4.5 Actual treatment:

The actual treatment which the patient received was as per institute protocol which was decided after careful consideration of clinical and imaging findings, co-morbidities and financial status of the patients. The treatment details including the type and number of the embolic agent used were recorded. The details of a number of attempts, treatment failure, and recurrence, were recorded. The immediate outcome of treatment at the time of discharge was also recorded.

4.6 Statistics:

Statistical analysis of the data was performed using IBM SPSS statistics 23.0 software**.** Quantitative variables were expressed as a mean ± standard deviation, and categorical variables were expressed as frequencies or percentages. Frequency measures were used for descriptive statistics.

Intermodality agreement and Kappa value was obtained for the two readers between the 2D DSA and 3D RA for the quantifiable characteristics.

Intermodality agreement and Kappa value was obtained for the two readers between the 2D DSA and 3D RA consensus reading for the quantifiable characteristics.

The descriptive characteristics were analyzed to look for improvement in detection of the quantifiable characteristics from 2D DSA to 3D RA evaluation**.** This was statistically evaluated by using the chi-square test to test the significance of improvement.

Interobserver agreement and Kappa value was obtained between the two readers for the assessment of quantifiable and descriptive characteristics on 2D DSA and 3D RA.

The agreement between the first treatment option and preferred embolic agent chosen on 2D DSA alone and combined 2D DSA and 3D RA by the two readers with that of the actual treatment was also calculated.

Interobserver agreement and Kappa value was obtained between the two readers for the choice of first treatment option and preferred embolic agent on 2D DSA and combined 2D DSA and 3D RA. Kappa value of ≤ 0 was considered as poor agreement, 0.01 - 0.20 as slight, 0.21 - 0.40 as fair agreement, 0.41 - 0.60 as moderate agreement, 0.61 - 0.80 as good and 0.81 - 1.00 as excellent agreement. $P < 0.05$ was considered statistically significant.

Results

5.1 Demographics:

The study included a total of 44 consecutive patients (40 male and four female; age range 17 - 65 years; mean [SD] 34.7 ± 13.5 years) with 45 traumatic CCF. 68 %(30 cases) of the cases were in the age group of 20 to 40 years. There were 13(30%) cases with the right, 30(68%) cases with left and one (2%) case with bilateral CCF.

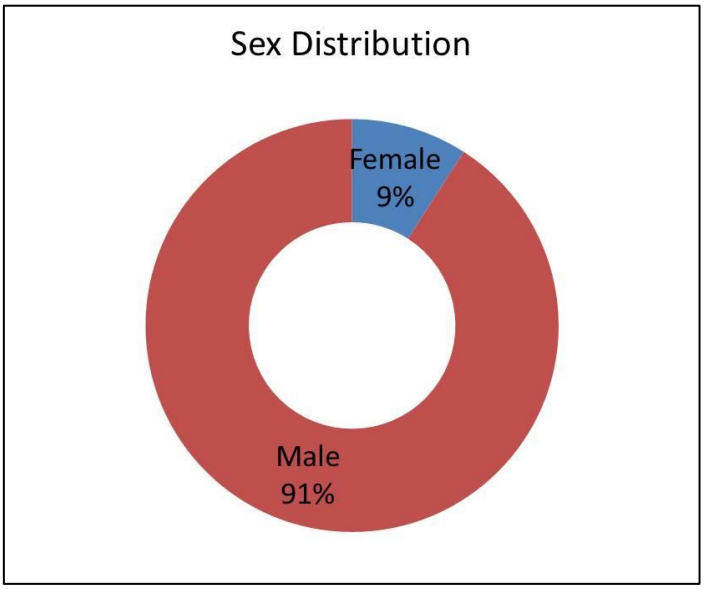

Figure 1: Sex distribution

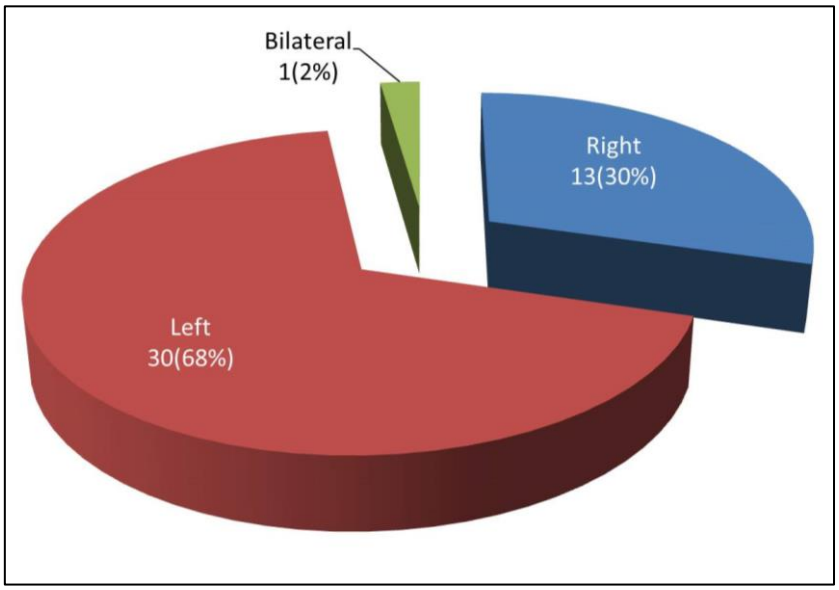

Figure 2: Side involved in 45 Carotid Cavernous Fistula.

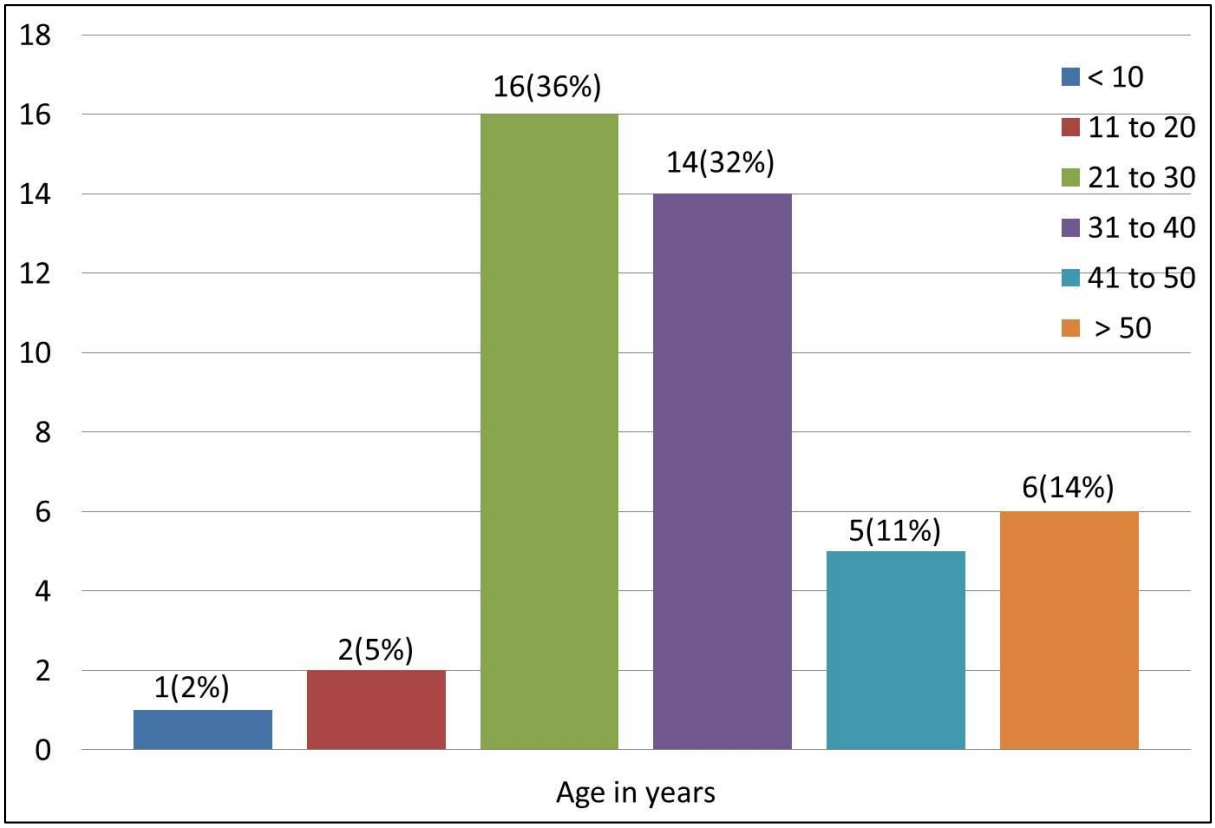

Figure 3: Age distribution

5.2 Clinical features:

Fifteen (34%) patients had right, twenty-four (53%) had left, and six (13%) had bilateral orbital/ocular symptoms at the time of presentation. Among the 44 cases, six cases had unilateral CCF with bilateral ocular/orbital symptoms at presentation, two patients had left sided CCF with contralateral ocular/orbital symptoms, and one patient had bilateral CCF with only right sided ocular/orbital symptoms.

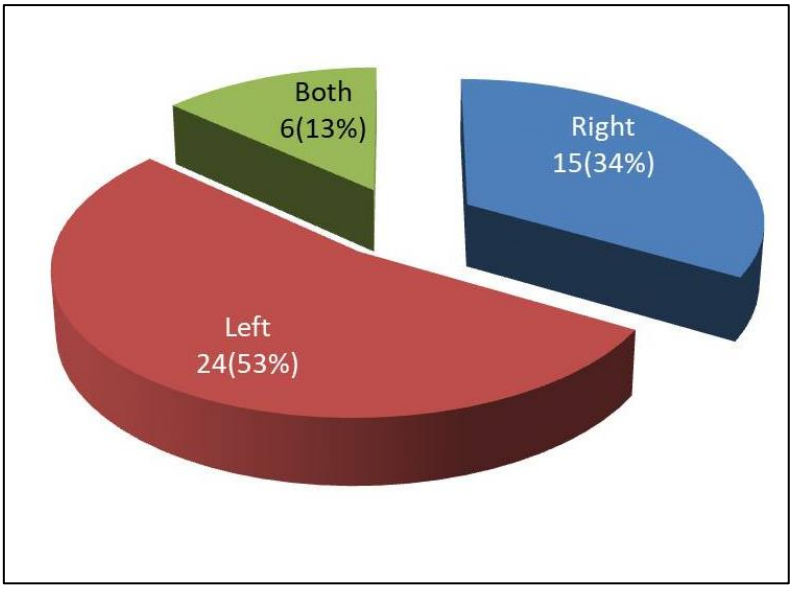

Figure 4: Side of eye involvement at the time of presentation

Orbital symptoms of proptosis, conjunctival congestion/chemosis, and periorbital swelling were the most common symptoms and was seen in 42(95%), 41(93%) and 38(86%) patients respectively. The other symptoms noted were orbital bruit in 33(75%), ophthalmoplegia in 31(70%), visual impairment in 22(50%), tinnitus in 16(36%) and diplopia in 17(39%) patients. Six (14%) patients developed isolated 6th nerve palsy, five (11%) developed isolated 3rd nerve palsy, eighteen (41%) developed both 3rd and 6th nerve palsy and 5th nerve palsy was seen in four (9%) patients. In 51% of the patients, clinical symptoms manifested within seven days of trauma whereas in 29% of the patients it took months to years to manifest. The IOP was elevated in 17 (38%) patients corresponding to the side of ocular symptoms. Six patients had a complete visual loss (PL or no PL) of which in two cases the visual loss was immediate following trauma.

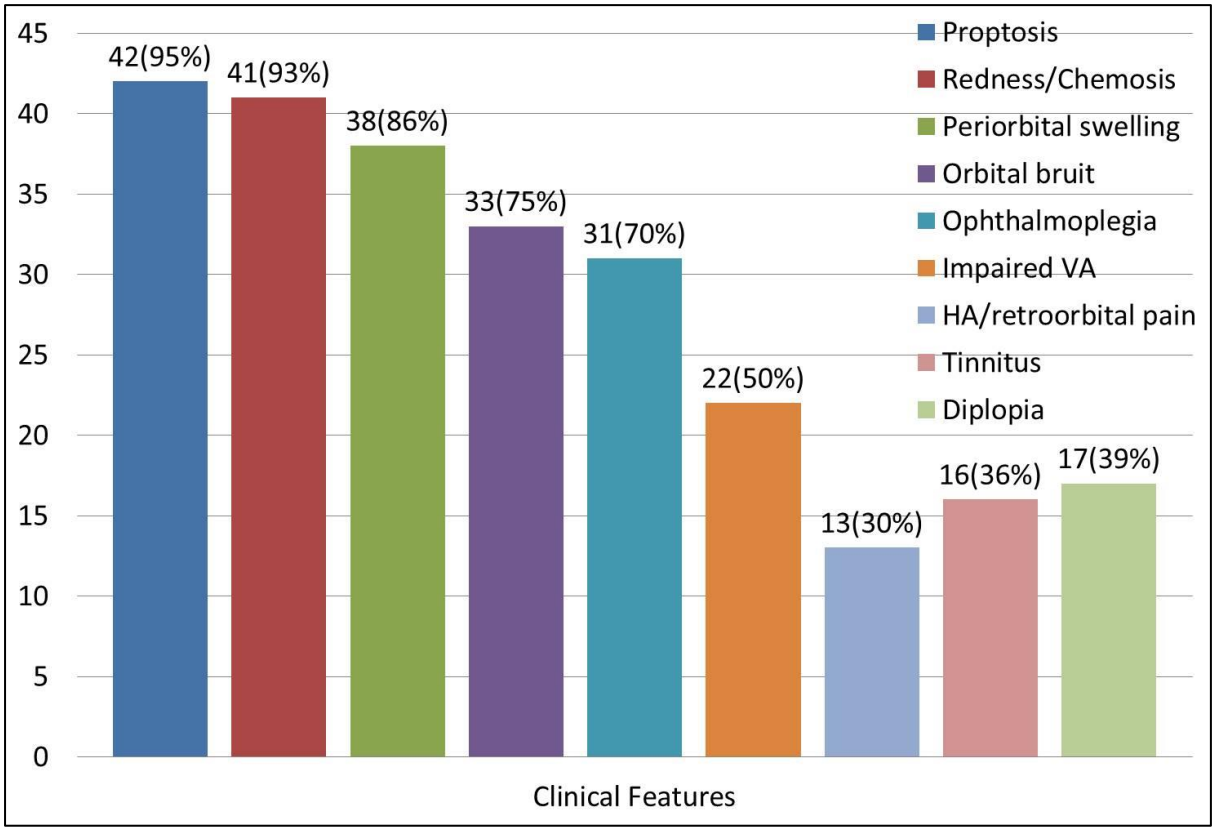

Figure 5: Clinical presentation

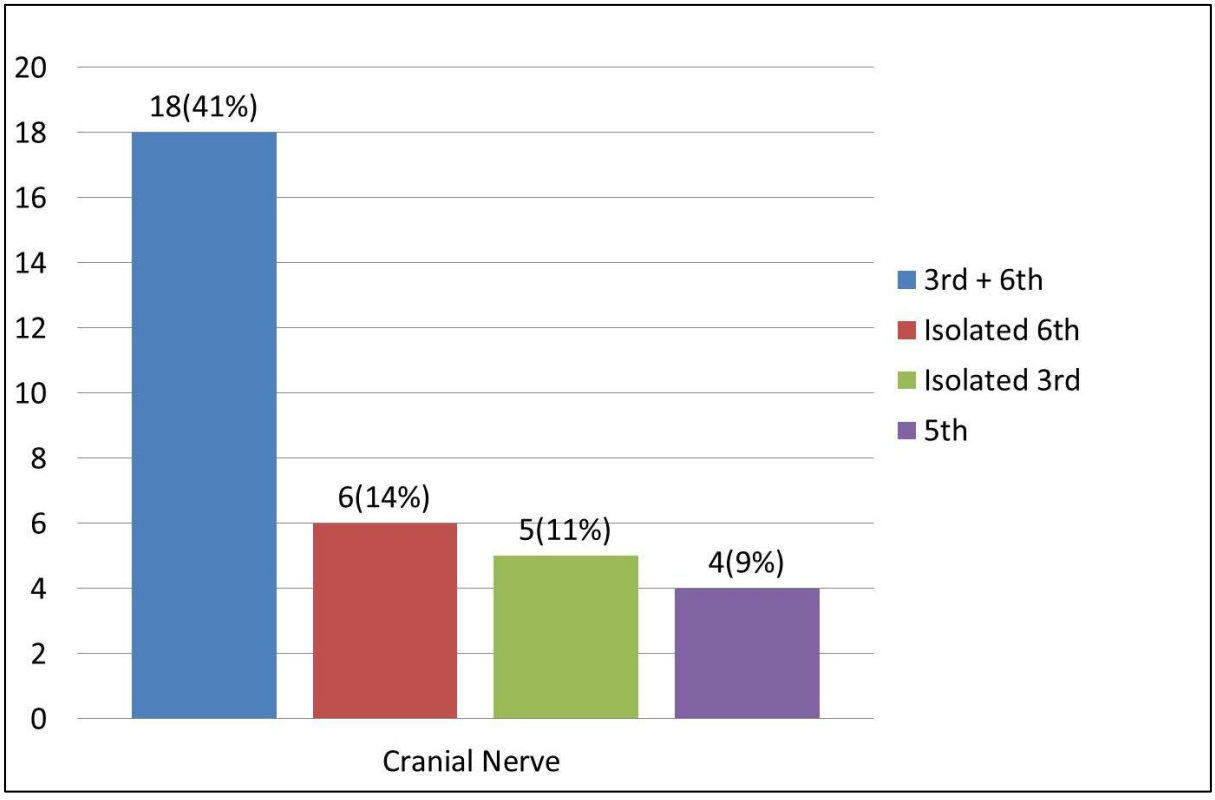

Figure 6: Cranial nerve involvement.

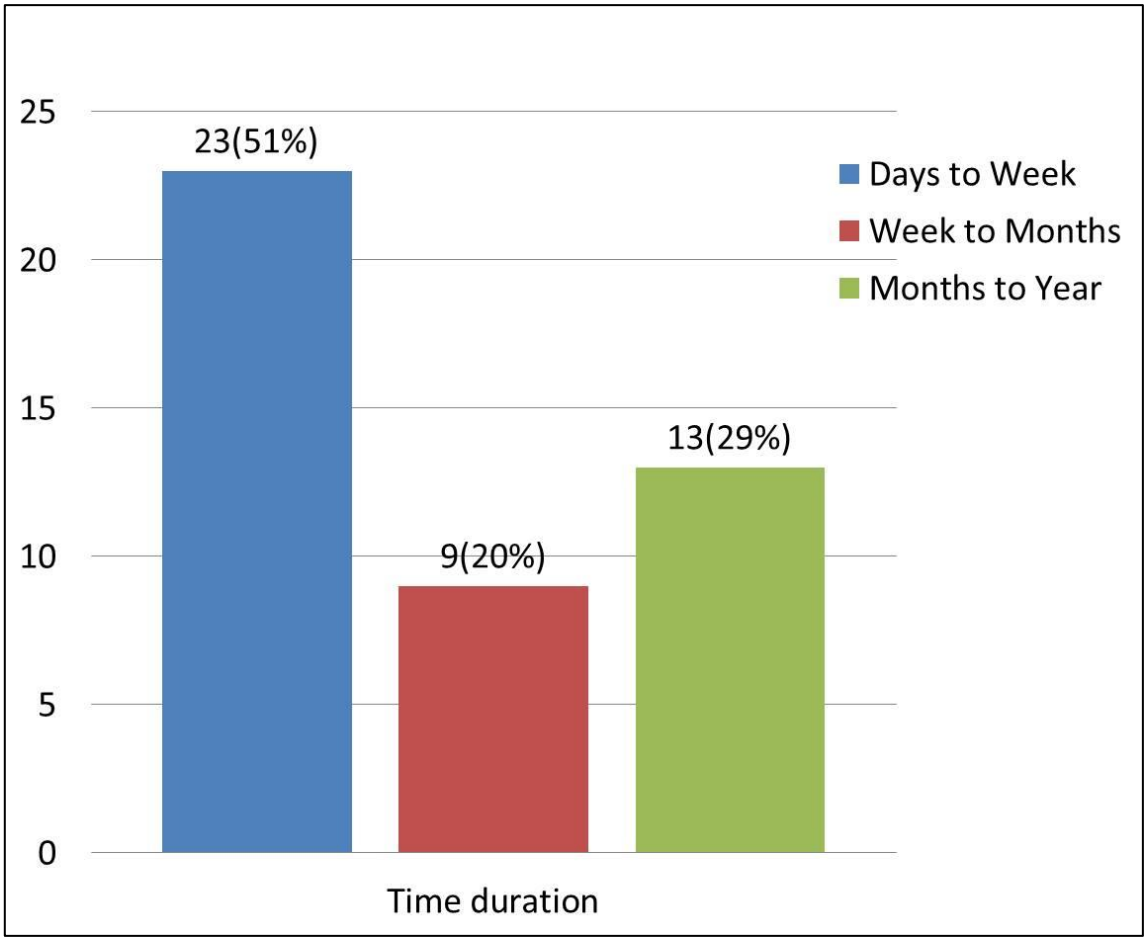

Figure 7: Time duration from RTA to initial clinical presentation

Skull base fracture was associated with 51 % of the CCFs, with anterior cranial fossa fracture in 11(25%) cases, middle cranial fossa in 9(20%) and posterior cranial fossa in 3(7%). 54 % (13) of the skull base fractures had an associated orbito maxillary fracture. Orbito maxillary fracture without skull base fracture was seen in 17% of the CCFs. In 28% of the traumatic CCFs, no associated skull base or orbitomaxillary fracture was noted. Intracranial haemorrhage associated with trauma was seen in 45% of CCFs. One patient a neglected traumatic CCF with neurofibromatosis type I developed acute deterioration caused by intracranial haemorrhage and intraventricular haemorrhage secondary to venous hypertension.

5.3 Angiographic characteristics: Size, number, and Location of fistula

Single fistula was seen in all 45 CCFs with the most common site being the posterior vertical segment [15/45 (33%)]. The location of fistula was in the posterior genu in 9 (20%) CCFs, horizontal segment in 8(18%), anterior genu in 8(18%) and anterior vertical segment in 5 (11%) CCFs.

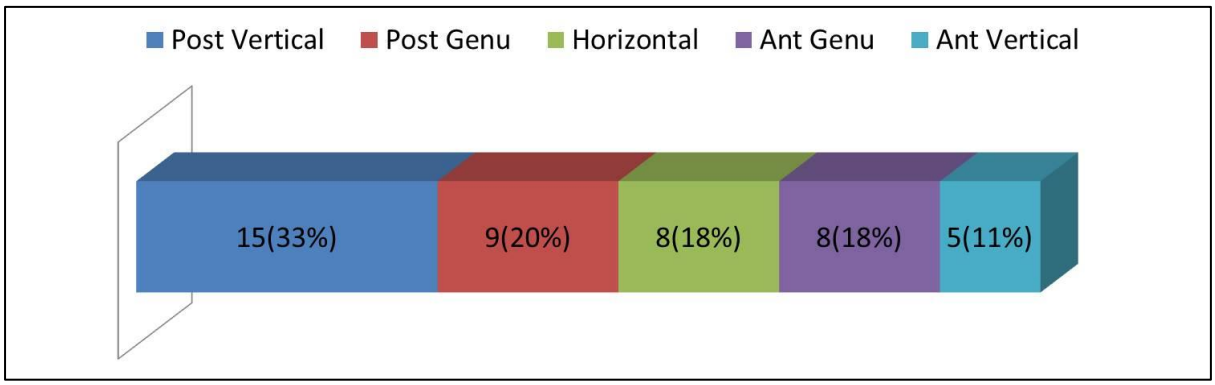

Figure 8: Location of Fistula

The rent of the fistula as measured on 3D RA ranged from 1.5 to 7 mm with mean [SD] of 3.9 mm[±1.3]. The fistula size could not be measured on 2D in 13(29%) CCFs. In 13(29%) CCFs, the size of the fistula measured on 2D matched with that of 3D or the difference was within ≤ 0.5 mm. In cases of discrepant measurements, 2D DSA underestimated the rent size in 17 (37%) and overestimated in 2(4%) cases.

Size of the rent measured on 2D versus 3D	No (%)
Size could not be measured on 2D	13(29%)
No difference or difference ≤ 0.5 mm	13(29%)
2D undersized the rent	17(38%)
2D oversized the rent	2(4%)

Table 1: Difference in size of the rent measured on 2D DSA versus 3D RA

The largest dimension of the of the first cavernous sac as measured on 3D RA ranged from 5 to 56 mm [mean 13.3 mm]. The larges cavernous sac measured was 56 x 38 mm, and the smallest sac size measured 5 x 3 mm. The size of the first cavernous sac measured on 2D matched with that of 3D or the difference was ≤ 1 cm in 16 (35%) CCFs. In 14 (31%) CCFs 2D undersized and in 15 (33%) CCF oversized the cavernous sac.

Size of the first cavernous sac measured on 2D versus 3D	No (%)
No difference or difference ≤ 1mm	16(36%)
2D undersized the cavernous sac	14(31%)
2D oversized the cavernous sac	15(33%)

Table 2: Difference in size of the first cavernous sac measured on 2D versus 3D

5.4 Venous drainage and CVR

Anterior, posterior and inferior venous drainage was seen in 16 (36%) CCFs anterior and posterior drainage in 16 (36%), anterior and inferior drainage in 3(6%), only anterior drainage in 8(18%) and only posterior drainage in 2(4%) CCFs. Cortical venous reflex was seen in 30 (67%) CCFs

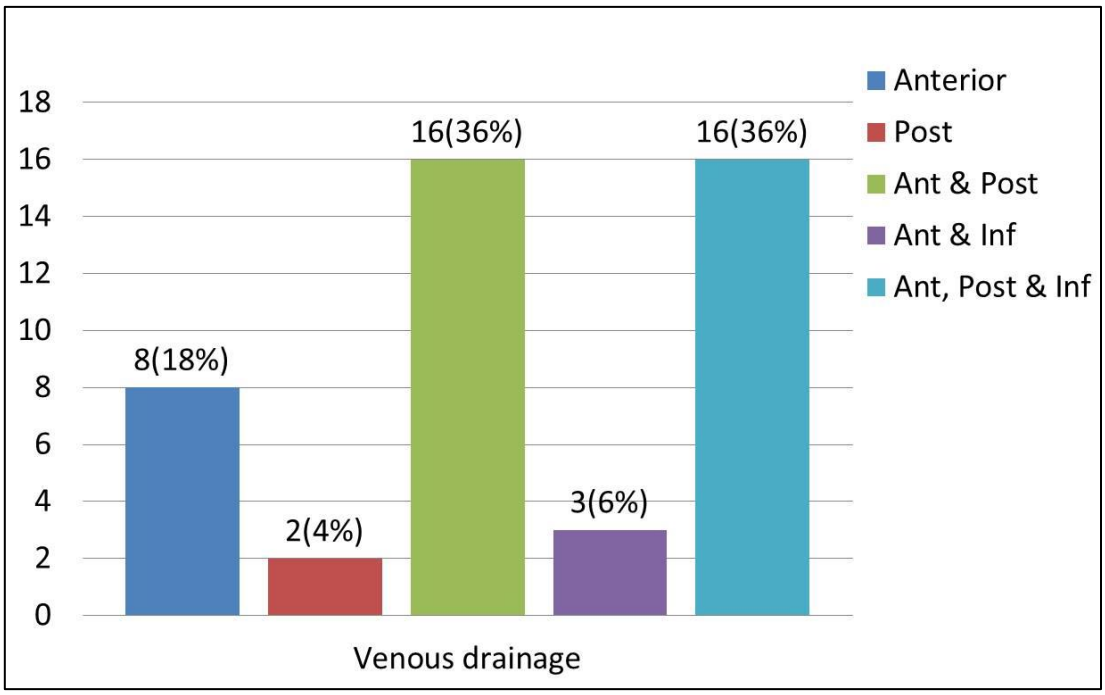

Figure 9: Venous Drainage

5.5.1 Subclassification on 2D DSA:

The CCFs on 2D DSA were subclassified into 16 (35%) small, 9 (20%) medium and 20 (44%) large-sized fistula. Of the 16 small size fistulas, 15 (94%) underwent reconstructive treatment, and one (6%) underwent deconstructive treatment. Of the nine medium-sized fistula eight (88%) underwent reconstructive treatment, and one (12%) underwent deconstructive treatment. Of the 20 large sized fistula six (30%) underwent reconstructive treatment and 14 (70%) underwent deconstructive treatment. In small-sized fistula,

detachable balloon embolization was done in seven (46%) CCFs and coil embolization in eight (53%) CCFs as reconstructive treatment. In medium sized fistula detachable balloon embolization was done in three (37%), coil embolization in four (50%) and stenting in one (13%) CCFs as reconstructive treatment. In large-sized fistula, detachable balloon embolization was done in six CCF as reconstructive treatment.

Subclassification on 2D DSA	**Balloon n (%)**	**Coils n (%)**
Small fistula (15)	7 (46%)	8 (53%)
Medium fistula (8)	3 (37%)	4 (50%)
Large fistula (6)	6 (100%)	

Table 3: Subclassification based on 2D DSA and embolic agent used

5.5.2 Subclassification on 3D:

The CCFs on 3D RA were subclassified into 25 (55%) small, 15 (33%) medium and 5 (11%) large-sized fistulas. Of the 25 small size fistulas, 19 (76%) underwent reconstructive treatment, and 6 (24%) underwent deconstructive treatment. Of the 15 medium sized fistulas, 9 (60%) underwent reconstructive treatment, and 6 (40%) underwent deconstructive treatment. Of the five large sized fistulas, 1 (20%) underwent reconstructive treatment, and 4 (80%) underwent deconstructive treatment. In small-sized fistula detachable balloon embolization was done in 9 (47%), coil embolization in 9 (47%) and stenting in 1 (6%) CCFs as reconstructive treatment. In medium sized fistula detachable balloon embolization was done in 6 (67%) and coil embolization in 3(33%) CCFs as reconstructive treatment. In large-sized fistula detachable balloon embolization was done in 1(100%) CCF as reconstructive treatment.

Subclassification on 3D	Balloon n (%)	Coils n (%)
Small fistula (19)	9 (47%)	9 (47%)
Medium fistula (9)	6 (67%)	3(33%)
Large fistula (1)	1 (100%)	

Table 4: Subclassification based on 2D DSA and embolic agent used

5.3 Quantifiable characteristics: Detection of location and number of rent:

	Reader 1	Reader 2
Location of rent	32 (71%) k = 0.619	22 (49%) k = 0.344
Number of rent	39	40

Table 5: Agreement between 2D DSA and 3D RA for reader 1 and reader 2

5.3.1 Reader 1 (Agreement between 2D DSA and 3D RA)

In the detection of the location of rent, the 2D DSA was concordant with 3D RA in 71% (32) of the CCFs (Kappa = 0.619; $p<0.001$). The discordance was more with the detection of the location in the posterior genu and posterior vertical segment in 3 (60%) and 5 (30%) CCFs respectively. In one case the location of the fistula which could not be identified on 2D DSA was identified on 3D DSA.

In the detection of the number of rent 2D DSA was concordant with 3D RA in 39 CCFs. The Kappa value could not be calculated as two by two contingency table was not possible.

5.3.2 Reader 2 (Agreement between 2D DSA and 3D RA)

In the detection of the location of rent, the 2D DSA was concordant with 3D RA in 49% (22) of the CCFs (Kappa =0.344; p<0.001). The discordance was more with the detection of the location in the posterior vertical segment, anterior vertical segment and posterior genu in 9 (81%), 2 (67%) and 6 (55%) CCFs

In the detection of the number of rent 2D DSA was concordant with 3D RA in 40 CCFs. The Kappa value could not be calculated as two by two contingency table was not possible

5.3.3 Reader 1 versus Reader 2 (for 2D DSA and 3D RA)

	2D DSA	3D RA
Location of rent	19 (42%) k =0.288	29 (64%) k =0 .556
Number of rent	39	40
Sub classification	33(73%) k = 0.604	32 (71%) k = 0 .527

Table 6: Agreement between reader 1 and reader 2 for 2D DSA and 3D RA.

2D DSA: In the detection of the location of the rent on 2D DSA reader one agreed with reader 2 in 42% (19) of the CCFs (Kappa =0.288; p<0.001). The concordance was for 3 CCFs in the posterior vertical segment, 3 in posterior genu, 9 in the horizontal segment, 3 in the anterior genu and 1 in the anterior vertical segment.

In the detection of the number of rent on 2D DSA reader 1 agreed with reader 2 in 39 CCFs

In the subclassification on 2D DSA reader 1 agreed with reader 2 in 73% (33) of the CCFs (Kappa = 0.604; p<0.001). The readers agreed for identifying small sized rent in 13 CCFs, medium sized 7 and large sized in 13 CCFs.

3D RA: In the detection of the location of the rent on 3D RA reader 1 agreed with reader 2 in 64% (29) of the CCFs (Kappa =0 .556; p<0.001). The concordance was for 11 CCFs in the posterior vertical segment, 5 in posterior genu, 7 in the horizontal segment, 4 in the anterior genu and 2 in the anterior vertical segment.

In the detection of the number of rent on 3D RA reader 1 agreed with reader 2 in 40 CCFs.

In the sub classification on 3D RA reader 1 agreed with reader 2 in 71% (32) of the CCFs (Kappa = 0 .527; p<0.001). The readers agreed in identifying small sized rent in 18 CCFs, medium sized 12 CCFs and large sized 2 CCFs

5.3.4 Agreement between 2D DSA and 3D RA consensus reading

	Reader 1	**Reader 2**
Location of rent	26 (56%) k = 0.46	19 (42%) k = 0.28
Number of rent	44	40

Table 7: Agreement b/w 2D DSA and 3D RA consensus reading for reader 1 and reader 2

Reader 1: In the detection of the location of rent the 2D DSA was concordant with 3D RA consensus reading in 56% (26) of CCFs(k = 0.46). The discordance was more with the detection of the location in the posterior genu in 9 (78%) and anterior genu in 4 (50%) CCFs. In one case the location of the fistula which could not be identified on 2D DSA.

In the detection of the number of rent 2D DSA was concordant with 3D RA consensus reading in 44 CCFs. The Kappa value could not be calculated as two by two contingency table was not possible.

Reader 2: In the detection of the location of rent the 2D DSA was concordant with 3D RA consensus reading in 42% (19) of CCFs (k = 0.28). The discordance was more with the detection of the location in the posterior vertical segment in 12 (80%), posterior genu in 6 (67%) and anterior vertical segment in 3 (60%) CCFs. In one case the location of the fistula which could not be identified on 2D DSA.

In the detection of the number of rent 2D DSA was concordant with 3D RA consensus reading in 40 CCFs. The Kappa value could not be calculated as two by two contingency table was not possible.

5.4 Additional angiographic findings:

There were three cases with pseudoaneurysm, one case with transection of the artery and one with dissection detected on 3D RA and one case of ectasia/dysplasia. In one case the sac was medially directed and was eroding the sphenoid sinus wall. All these findings were not identified on 2D RA

5.5 Descriptive Characteristics: Quality of detection of size, number, and location

5.5.1 Reader 1: For the detection of the location of the rent the mean quality was good to sufficient (score, 1.933) for 2D DSA and good (score, 1.000) for 3D RA with improvement in the quality of response for assessment made on combine 2D DSA and 3D RA (P <0.001).

For the detection of the number of rent the mean quality was sufficient to insufficient (score, 2.067) for 2D DSA and good (score, 1.000) for combine 2D DSA and 3D RA with improvement in quality of response for assessment made on combine 2D DSA and 3D RA (P <0.001)

For determination of the size of rent the mean quality was sufficient to insufficient (score, 2.267) for 2D DSA and good (score, 1.000) for combine 2D DSA and 3D RA with improvement in quality of response for assessment made on combine 2D DSA and 3D RA (P <0.001)

5.5.2 Reader 2: For the detection of location or rent the mean quality was good to sufficient (score, 1.844) for 2D DSA and good to sufficient (score, 1.067) for combine 2D DSA and 3D RA with improvement in quality of response for assessment made on combine 2D DSA and 3D RA (P <0.001).

For the detection of the number of rent the mean quality was good to sufficient (score, 1.978) for 2D DSA and good to sufficient (score, 1.111) for combine 2D DSA and 3D RA with improvement in quality of response for assessment made on combine 2D DSA and 3D RA (P <0.001)

For determination of the size of the rent the mean quality was good to sufficient (score, 1.756) for 2D DSA and good to sufficient (score, 1.067) for combine 2D DSA and 3D RA with improvement in quality of response for assessment made on combine 2D DSA and 3D RA (P <0.001)

5.6.1 Therapeutic planning: (First treatment option)

Reader 1 on 2D DSA correctly predicted therapeutic plan as constructive in 28 (65%) CCFs and as destructive in 1 (50%) CCFs (k = 0.035; p = 0.662)

		Actual treatment		
		Constructive	Destructive	
First treatment option chosen on 2D	Constructive	28 (65%)	15 (35%)	43
	Destructive	1 (50%)	1 (50%)	2
		29	16	45

Table 8: Therapeutic plan based on 2D DSA compared with actual treatment

Reader 1 on combined 2D DSA and 3D RA correctly predicted therapeutic plan as constructive in 27 (73%) CCFs and as destructive in and destructive in 6 (75%) CCFs (k = 0.345; p = 0.010).

		Actual treatment		
		Constructive	Destructive	
First treatment option chosen on 2D + 3D	Constructive	27 (73%)	10 (27%)	37
	Destructive	2 (25%)	6 (75%)	8
		29	16	45

Table 9: Therapeutic plan based on combined 2D DSA & 3D RA compared with actual treatment.

The mean quality was good to sufficient (score, 1.911) for 2D DSA and good to sufficient (score, 1.022) for combined 2D DSA and 3D RA with improvement in the quality of response for assessment made on combine 2D DSA and 3D RA (P <0.001).

Reader 2 on 2D DSA correctly predicted therapeutic plan as constructive in 28 (80%) CCFs and as destructive in 9 (90%) (k = 0.576 p < 0.001).

		Actual treatment		
		Constructive	Destructive	
First treatment option chosen on 2D	Constructive	28 (80%)	7 (20%)	35
	Destructive	1 (10%)	9 (90%)	10
		29	16	45

Table 10: Therapeutic plan based on 2D DSA compared with actual treatment

Reader 2 on combined 2D DSA and 3D RA correctly predicted therapeutic plan as constructive in 29 (83%) and as destructive in 10 CCFs (k = 0.682; p < 0.001).

		Actual treatment		
		Constructive	Destructive	
First treatment option chosen on 2D + 3D	Constructive	29 (83%)	6 (17%)	35
	Destructive	0	10 (100%)	10
		29	16	45

Table 11: Therapeutic plan based on combine 2D + 3D RA compared with actual treatment

The mean quality was good to sufficient (score, 1.667) for 2D DSA and good to sufficient (score, 1.044) for combine 2D DSA and 3D RA with improvement in the quality of response for combined assessment made on 2D DSA and 3D RA (P <0.001).

The interobserver agreement between R1 and R2 for the choice of first treatment option based on 2D DSA alone and combine 2D DSA, and 3D RA was fair (Kappa 0. 100 p = 0.334) and moderate (Kappa: 0.585; p < 0.001) respectively.

5.6.2 Therapeutic planning: (Preferred embolic agent)

Reader 1 on 2D DSA correctly predicted preferred embolic agent as balloon in 15 (75%) and coil in 6 (75%) CCFs (k = 0. 479; p = 0.005)

		Actual agent used			
		Balloon	Coil	Stent	
Preferred embolic agent chosen on 2D + 3D	Balloon	15 (75%)	5	0	20
	Coil	1	6 (75%)	1	8
		16	11	1	28

Table 12: Embolic agent chosen based on 2D DSA compared with actual treatment

Reader 1 on combined 2D DSA and 3D RA correctly predicted preferred embolic agent as balloon in 12 (80%) and coil in 8 (67%) CCFs (k = 0.492; p = 0.007).

		Actual agent used			
		Balloon	Coil	Stent	
Preferred embolic agent chosen on 2D	Balloon	12 (80%)	3	0	15
	Coil	3	8 (67%)	1	12
		15	11	1	27

Table 13: Embolic agent chosen based on combined 2D DSA and 3D RA

The mean quality was good to sufficient (score, 1.946) for 2D DSA and good (score, 1.000) for combine 2D DSA and 3D RA with improvement in the quality of response for combined assessment made on 2D DSA and 3D RA (P <0.001).

Reader 2 on 2D DSA correctly predicted preferred embolic agent as balloon in 8 (62%) of CCFs and coil in 8 (53%) of CCFs. (k = 0. 178; p = 0.3).

		Actual agent used			
		Balloon	Coil	Stent	
Preferred embolic agent chosen on 2D	Balloon	8 (62%)	4	1	13
	Coil	7	8 (53%)	0	15
		15	12	1	28

Table 14: Embolic agent chosen based on 2D DSA compared with actual treatment

Reader 2 on combined 2D DSA and 3D RA correctly predicted preferred embolic agent as balloon in 13 (87%) and coil in 10 (71%) CCFs (k = 0. 598; p = 0.001)

		Actual agent used			
		Balloon	Coil	Stent	
Preferred embolic agent chosen on 2D + 3D	Balloon	13 (87%)	2	0	15
	Coil	3	10 (71%)	1	14
		16	12	1	29

Table 15: Embolic agent chosen based on combined 2D DSA and 3D RA

The mean quality was good to sufficient (score, 1.750) for 2D DSA and good (score, 1.156) for combine 2D DSA and 3D RA with improvement in the quality of response for combined assessment made on 2D DSA and 3D RA (P <0.001).

The interobserver agreement between R1 and R2 for the choice of preferred embolic agent based on 2D DSA alone and combined 2D DSA and 3D RA was poor (Kappa .093; p = 0. 551) and fair (Kappa 0.311; p = 0.073) respectively.

5.7 Subclassification on 3D:

The angle of a sector of defect measured at the site of the fistula on 3D RA was significantly higher for deconstructive treatment compared to the constructive treatment (p< 0.001). 75% of the angles were below 95°to 100° when the CCF was treated with constructive treatment whereas 75% of the angles were above 95°to 100° when the CCF was treated with destructive treatment.

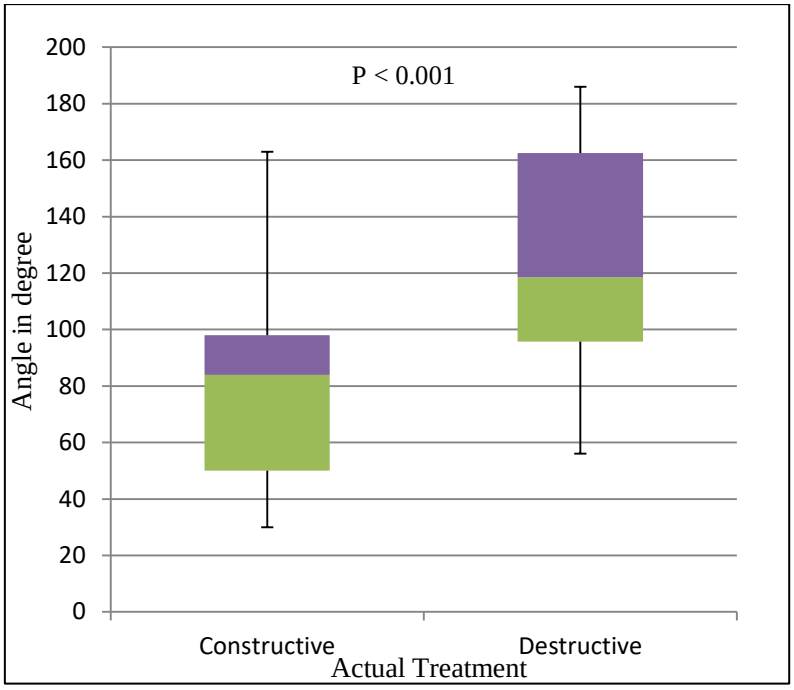

Figure 10: Relation between the sector of defect and treatment option

The distribution of the angles was lower when coils were used for treatment as compared to the cases when balloons were used for treatment though this was not statistically significant.

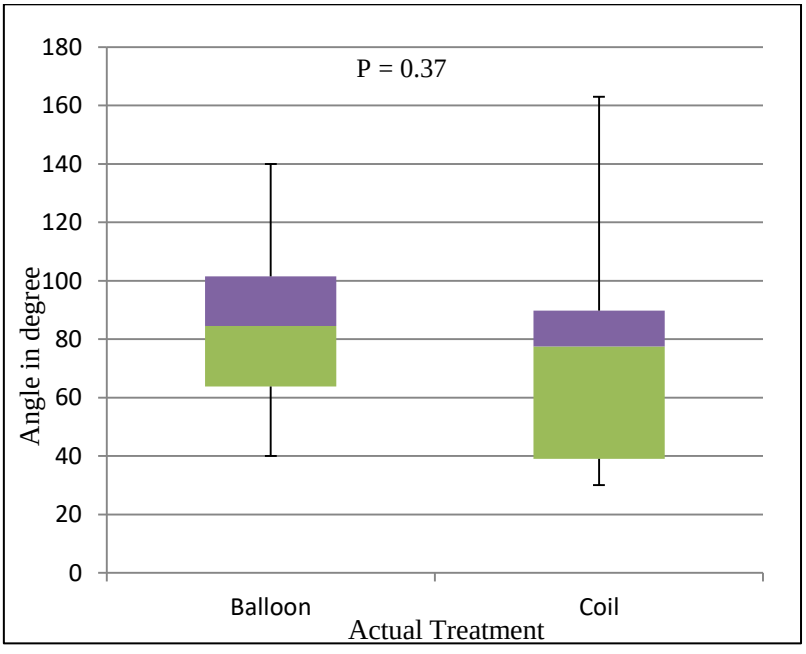

Figure 11: Relation between the sector of defect and embolic agent

5.8 Actual treatment:

Endovascular treatment was done for 45 CCFs of which 29(64%) underwent the reconstructive procedure, and 16(35%) underwent the deconstructive procedure in the form of PAO. The embolic agent used for the reconstructive procedure was as follows: a detachable balloon in 16(55%), detachable coils in 12(41%) and covered stent in 1(3%). A supplementary embolic agent like NBCA and EVOH copolymer where used in 7 cases, in 5 cases (3: NBCA; 1: Squid; 1: Onyx) it was used along with coils for PAO and in two cases along with transarterial venous sac coiling.

Of the 45 CCFs treated with endovascular intervention, 9 (20%) CCFs required more than one sitting with up to two sittings done for 7 (15%) CCFs and three sittings in 2(4%) CCFs either due to treatment failure or recurrence.

.

Failure: There were 7 CCFs with treatment failure from the use of the balloon either due to difficulty in navigability of the balloon (n = 2), difficulty in obtaining cessation of flow (n = 3), parent artery compromise on balloon inflation (n = 1) or migration of balloon into SOV (n = 1). In one CCF the treatment failed even on the second attempt with balloon and coils. Of these 7 CCFs with treatment failure one underwent stenting, two underwent coiling, and 4 CCFs underwent PAO as a final intervention.

Recurrence: There were four CCFs with recurrence after embolization with a detachable balloon due to premature balloon deflation. Two of these recurrences were treated with PAO, one with coiling and one with repeat balloon embolization. Four patients who were treated with PAO developed recurrence. Among these two were due to recanalization of the occlude ICA secondary to the development of vaso-vasorum or recanalization of the occluded segment with the simultaneous recruitment of dural feeder. Both these cases were treated

with transvenous coiling. In two CCFs the recurrence was through the retrograde filling of the fistula as only proximal ICA occlusion was not done in the initial sitting. Both these cases were treated with distal ICA coiling via PCOM.

Complication: No major morbidity or mortality was noted. One case of stuck microcatheter with failure to detach the balloon and one case of extravasation from inferior epigastric artery during the procedure was observed.

Case 1: **Recurrence of traumatic carotid cavernous fistula after parent artery occlusion**

A 55-year-old male was involved in a RTA and sustained a head injury. Computed tomography showed fractures involving the left temporal bone and left the orbital wall. He developed insidious onset redness and proptosis in left eye two weeks after RTA, which was suspected to be CCF. MRI showed the prominence of the left CS and bilateral SOV. DSA confirmed the presence of direct CCF in left cavernous ICA and a pseudoaneurysm of the left MMA.

1st Intervention: Endovascular intervention with PAO for left direct CCF and coil embolization of left MMA pseudoaneurysm. PAO was performed using detachable coils, and an immediate post-intervention check angiogram revealed complete cessation of the shunt.

Recurrence: He was asymptomatic for the next five months when his symptoms of left eye proptosis and redness recurred. Check DSA was revealed recurrence of the CCF on the left side. The arterial feeders were from distal branches of left internal maxillary, clival branches of left ascending pharyngeal arteries and left MMA. Minimal supply from distal branches of right IMA and meningiohypophyseal branches of right ICA was also noted. The left ICA showed recanalization through vasa vasorum, which was also contributing to the fistula.

2nd Intervention: Transvenous embolization the left CS was performed with coils and Squid 18 liquid embolic device, achieving complete obliteration of the sac and cessation of the shunt. Check angiogram done 5 days post-intervention showed no evidence of residual fistula. He remained asymptomatic till last clinical follow-up at two years.

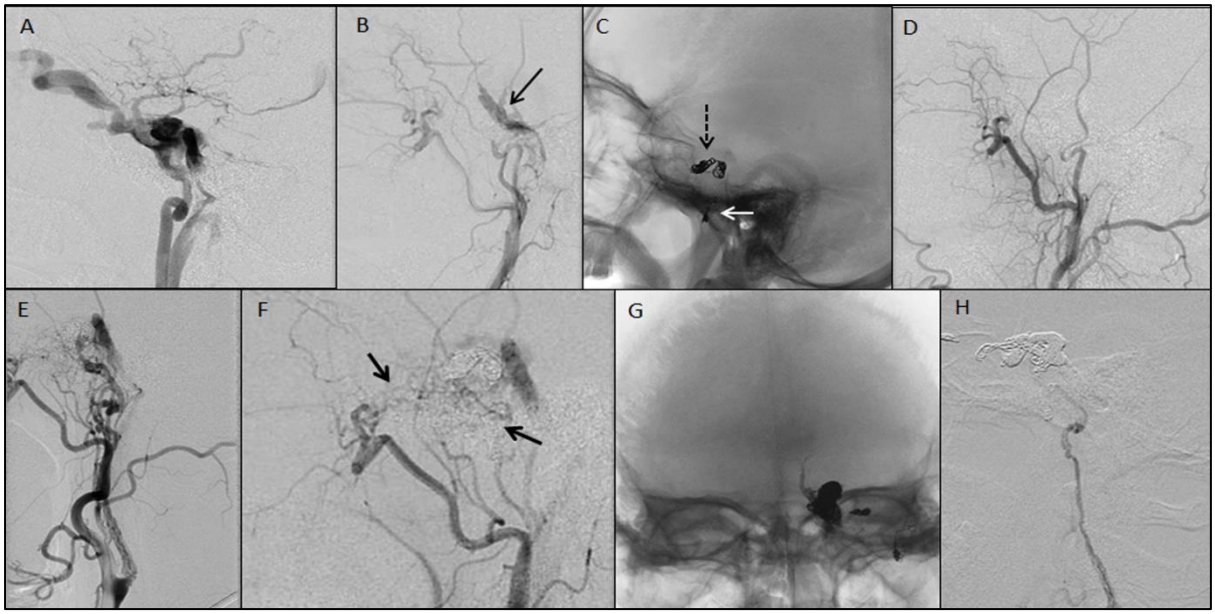

Fig 1: Angiogram and intervention during the initial presentation (A –D). Left ICA angiogram, (A) Lat view showing direct CCF with anterior and posteroinferior venous drainage and cortical venous reflux. Left ECA angiogram (B) Lat view showing traumatic pseudoaneurysm of the MMA(Black arrow). Radiography of Skull (C) AP view showing coil mass of PAO in the left para sellar region(dashed black arrow) and MMA pseudoaneurysm embolization in the left middle cranial fossa(white arrow). Left CCA angiogram post-embolization (D) Lat view is showing a complete cessation of the shunt and no opacification of the left ICA. Angiogram and intervention during the recurrence. Left CCA angiogram, (E) Lat view showing recurrence of the left CCF with recanalization of the ICA via vaso vasorum(Black arrow). Left ECA angiogram, (F) Lat view showing distal IMA and MMA branches contributing to the fistula(Black arrows). Radiograph of the skull (G) showing coil mass and Squid cast in the left para sellar region from transvenous embolization of the left cavernous sinus(dashed white arrow). Left CCA angiogram post embolization, (H) Lat view showing a complete cessation of the shunt with persistent opacification of the vaso vasorum.

Case 2: **Recurrence of traumatic carotid cavernous fistula after parent artery occlusion**

A 25-year-old male was involved in an RTA and sustained maxillofacial and head injuries. One day later, he developed pulsatile proptosis and chemosis in the right eye. CT scan showed prominent bilateral SOV, and mandibular fracture and DSA examination revealed a right direct CCF.

1st Intervention: Underwent detachable balloon embolization of the venous sac, however, due to the protrusion of the balloon through the rent into the parent artery and resultant flow compromise, PAO was considered to avoid thromboembolic complications. PAO was performed using detachable coils. Post-procedure period, he had good symptomatic improvement with subsequent resolution of his proptosis and chemosis.

Recurrence: On 17th post procedure day, he developed recurrence of right eye proptosis and chemosis which gradually progressed. Follow up DSA showed recurrence of his right CCF with supply anterogradely from the recanalized right ICA as well as from the terminal branches of bilateral IMA**.**

2nd Intervention: Transvenous coiling of the right CS was done resulting in complete cessation of the shunt.

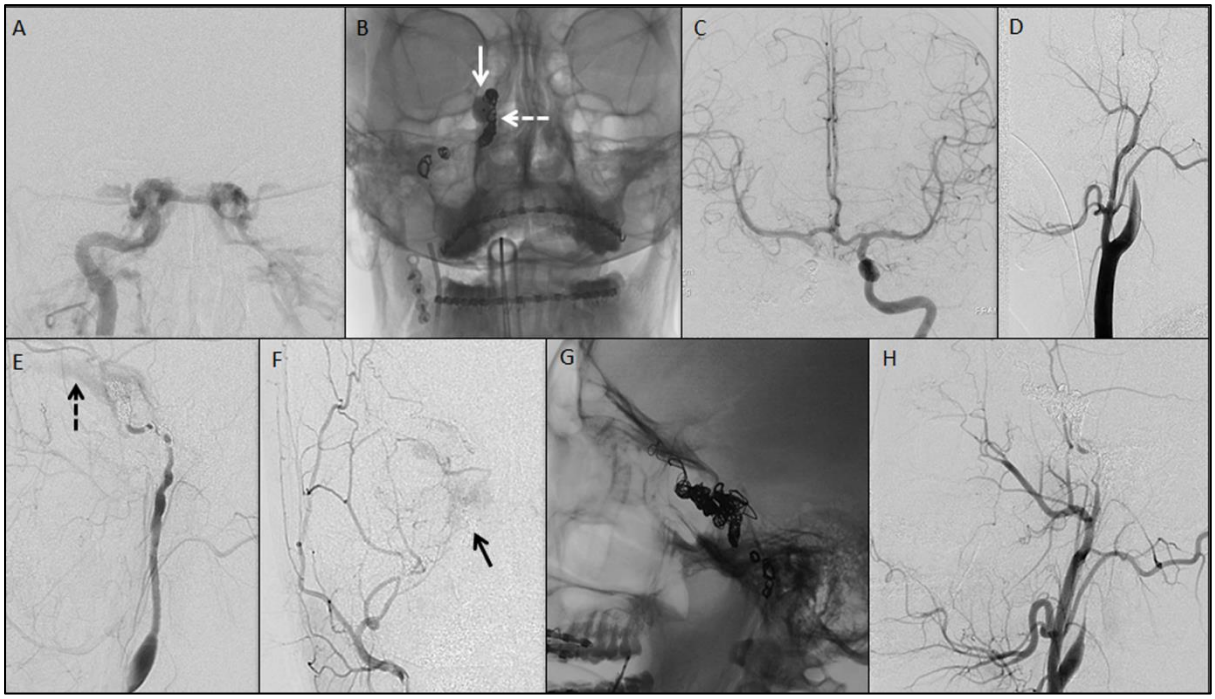

Fig 2: Angiogram and intervention during initial presentation. Right ICA angiogram, (A) AP views showing direct CCF with anterior and posteroinferior venous drainage. Radiography of Skull (B) AP view showing detachable balloon in the cavernous sinus(white arrow) with coil mass of PAO in the right para sellar region(Dashed white arrow). Left ICA angiogram post-embolization (C) AP view showing a complete cessation of the shunt. Right, CCA angiogram (D) Lat view is showing a complete termination of the shunt and no opacification of the right ICA. Angiogram and intervention during the recurrence. Right CCA angiogram, (E) Lat views showing recurrence of the left CCF with recanalization of the ICA. SOV (Dashed black arrow). Right ECA angiogram, (F) AP view showing distal IMA branches contributing to the fistula(Black arrow). Radiograph of the skull (G) Lat view showing coil mass in the right para sellar region from transvenous embolization of the right cavernous sinus. Right CCA angiogram, (H) Lat view showing a complete cessation of the shunt and no opacification of the right ICA.

Case 3: Traumatic CCF with Pseudoaneurysm eroding the sphenoid sinus

A 29-year-old male was involved in a road traffic accident and developed loss of vision in the left eye. Post-trauma he also developed CSF rhinorrhoea and left periorbital swelling which on evaluation revealed CCF. DSA revealed a left CCF with large venous sac/pseudoaneurysm projecting into the sphenoid sinus.

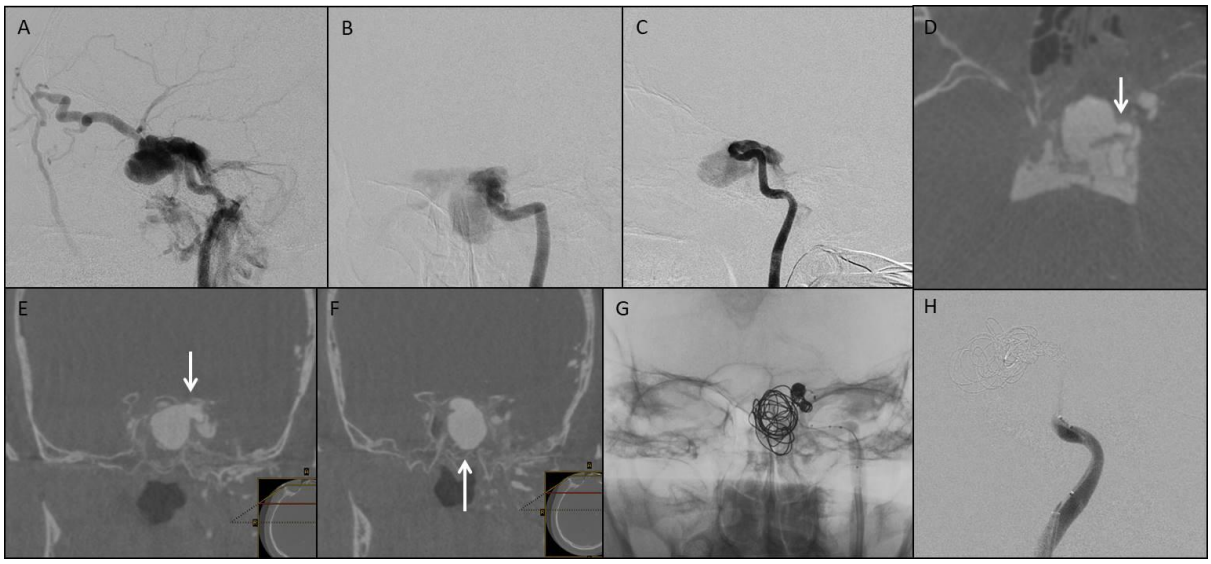

Fig 3: Left ICA angiogram, (A) Lat & (B) AP views showing direct CCF with anterior and posteroinferior venous drainage and a large medial venous sac. (C) Mehringer-Hieshima manoeuvre showing the location of the fistula in the anterior vertical segment with a venous sac. 3D RA axial (D) & Coronal (E) & (F) Rent along the medial aspect of the anterior vertical segment (white arrow in D & E) and large venous sac/pseudoaneurysm eroding the sinus wall. Radiograph of Skull (G) Coiling of the venous sac/pseudoaneurysm and left cavernous ICA proximal to the fistula. Left CCA angiogram, (H) Lat views Stasis of flow in the right ICA with complete cessation of the shunt and occlusion of the ICA.

Case 4: Right direct CCF managed with stenting of the ICA

A 57-year-old female with a history of RTA, developed proptosis, redness, periorbital oedema and impaired vision in the right eye. DSA revealed a right direct CCF. She underwent failed attempts of embolization with balloon and coils. Subsequently stenting of the ICA (Jostent 3.5 x 12 mm)

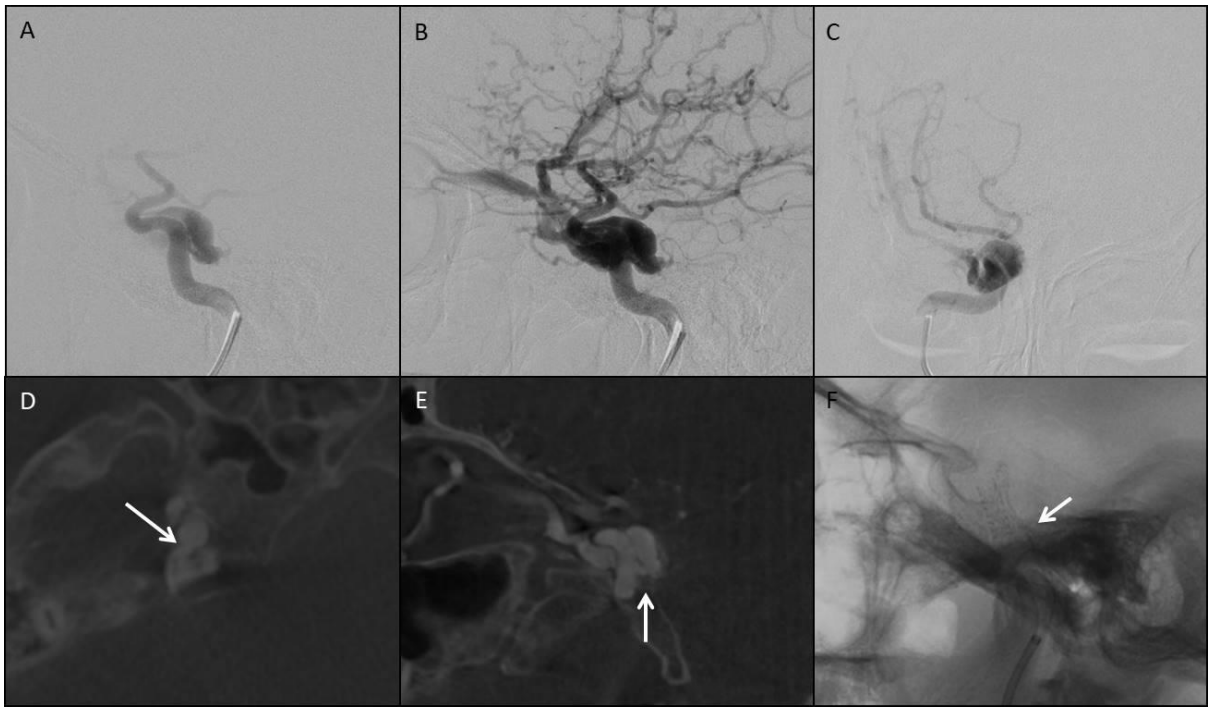

Fig 4: Right ICA angiogram, (A), (B) & (C) AP & Lat views showing direct CCF with small fistula and anterior venous drainage. Mehringer-Hieshima (A) manoeuvre showing the location of the fistula in the posterior vertical segment along the posterior wall. 3D RA axial (D) & Sagittal (E) Rent along the posterior aspect of the posterior vertical segment (white arrow). Radiograph of Skull (F) Lat view, Jostent (3.5 x 12 mm) in the right cavernous ICA.

Case 5: Right CCF with transection of artery treated with PAO

A 37-year-old male involved in a motor vehicle accident. Developed tinnitus four days post-trauma. Subsequently developed, proptosis, progressive redness, and swelling of both eyes with diplopia. DSA revealed right direct CCF. Initially, balloon attempted but failed and the procedure converted to PAO.

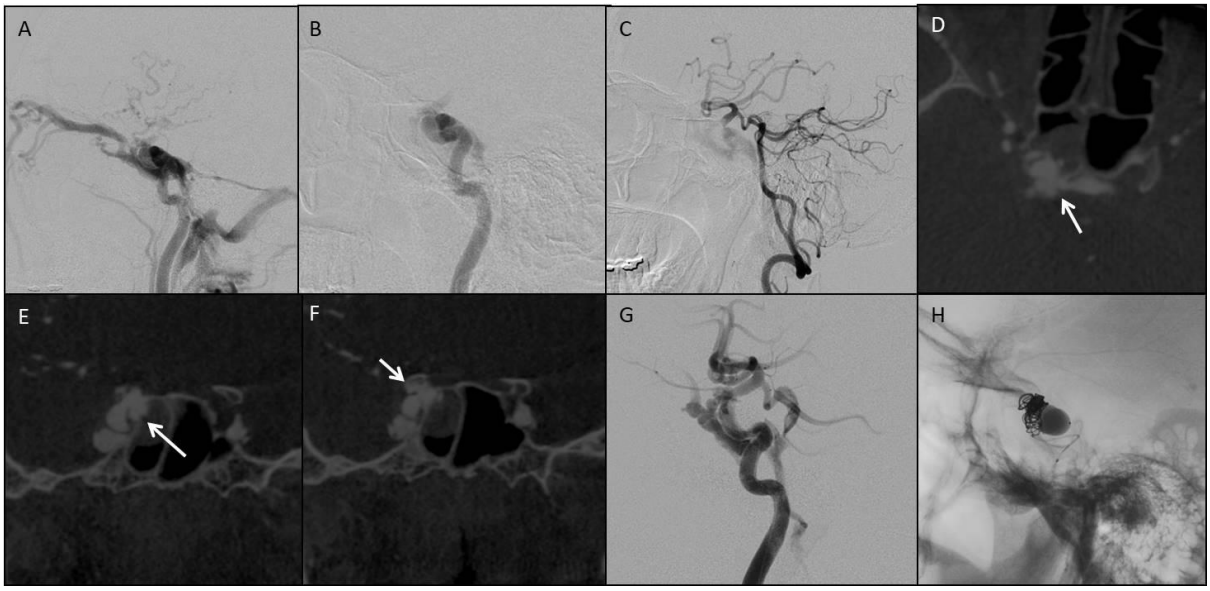

Fig 5: Right ICA angiogram, (A) & (B) Lat views showing direct CCF with large fistula and anterior and posterior venous drainage with cortical venous reflux. Mehringer-Hieshima (B) manoeuvre not able to localize the rent. Heuber manoeuvre (C) showing the location of the fistula in the anterior vertical segment. 3D RA axial (D) & Coronal (E) Defect along the anterior and posterior wall of anterior vertical segment suggestive of transection (white arrow). Right ICA angiogram (G) Golbal 4 balloon inflated in the cavernous sac with a persistent shunt. Radiograph of Skull Lat view (H) PAO done with the inflated balloon in cavernous sac and coil mass in ICA.

Case 6: Left CCF with Pseudoaneurysm managed with transarterial coiling

A 28-year-old male involved in road traffic accident. Developed pulsatile proptosis with periorbital swelling in the left eye. DSA revealed a left direct CCF.

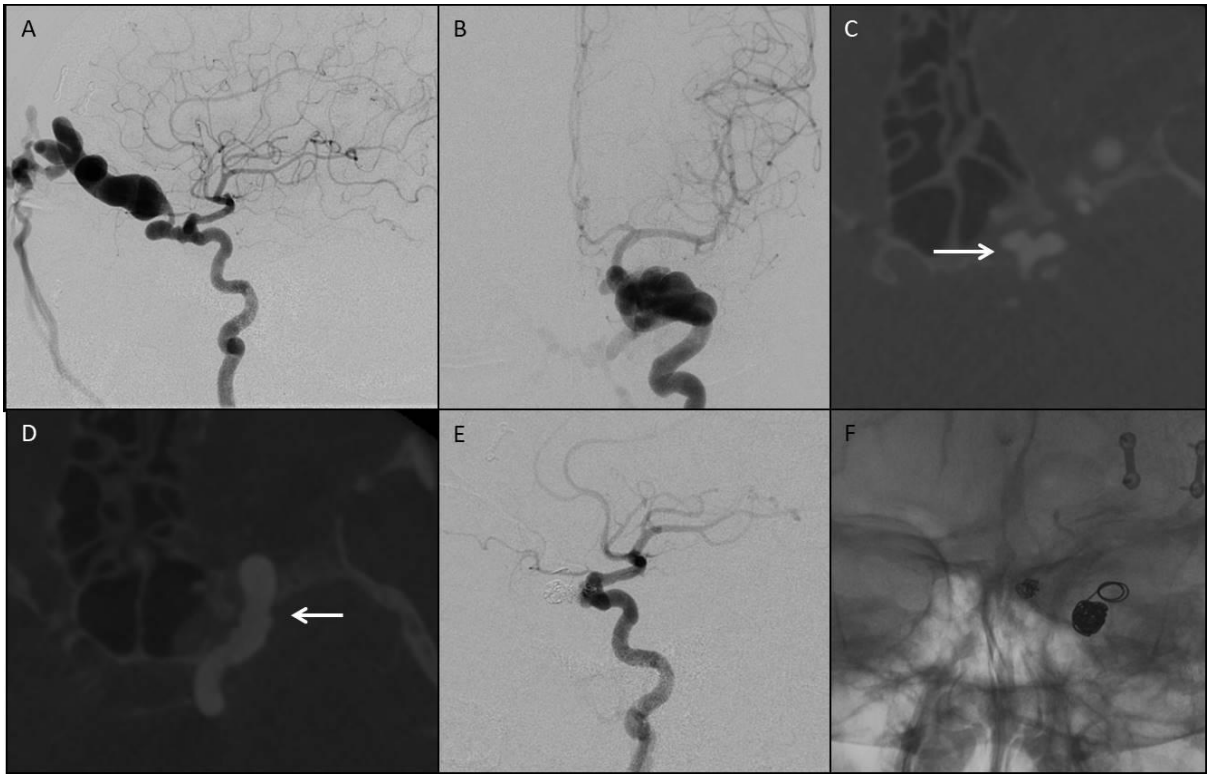

Fig 6: Left ICA angiogram, (A) & (B) AP & Lat views showing direct CCF with small fistula and anterior venous drainage. 3D RA axial (C) & (D) Defect along the anterior aspect of the anterior genu (white arrow in D). There is a small pseudoaneurysm directed medially. Left ICA angiogram post coil embolization (E) coil embolization of the pseudoaneurysm and the venous sac with complete cessation of the shunt. Radiograph of the skull AP view (F) Coil mass in the venous sac and pseudoaneurysm.

Case 7: Left Direct CCF with left cavernous ICA dysplasia.

A 27-year-old male involved in RTA sustained left central skull base and maxillofacial fracture. Later developed swelling, proptosis, and chemosis of the left eye. DSA revealed left direct CCF with ectasia and dysplasia of the cavernous ICA. Underwent PAO.

Fig 7: Left ICA angiogram, (A) & (B) AP & Lat views showing direct CCF with anterior and inferior venous drainage and cortical venous reflex. 3D RA axial (C) & Coronal (D) shows defect along the anterior and lateral aspect of the posterior vertical segment (white arrow) with ectasia of the cavernous ICA. Left ICA angiogram post coil embolization (E) reveals stasis of flow in the left ICA with PAO. Radiograph of the skull AP view (F) Coil mass in the left ICA.

Case 8: Right direct CCF underwent transarterial coiling.

A 60-year-old male involved in an RTA presented with complains of visual loss and redness of the right eye. DSA revealed right direct CCF.

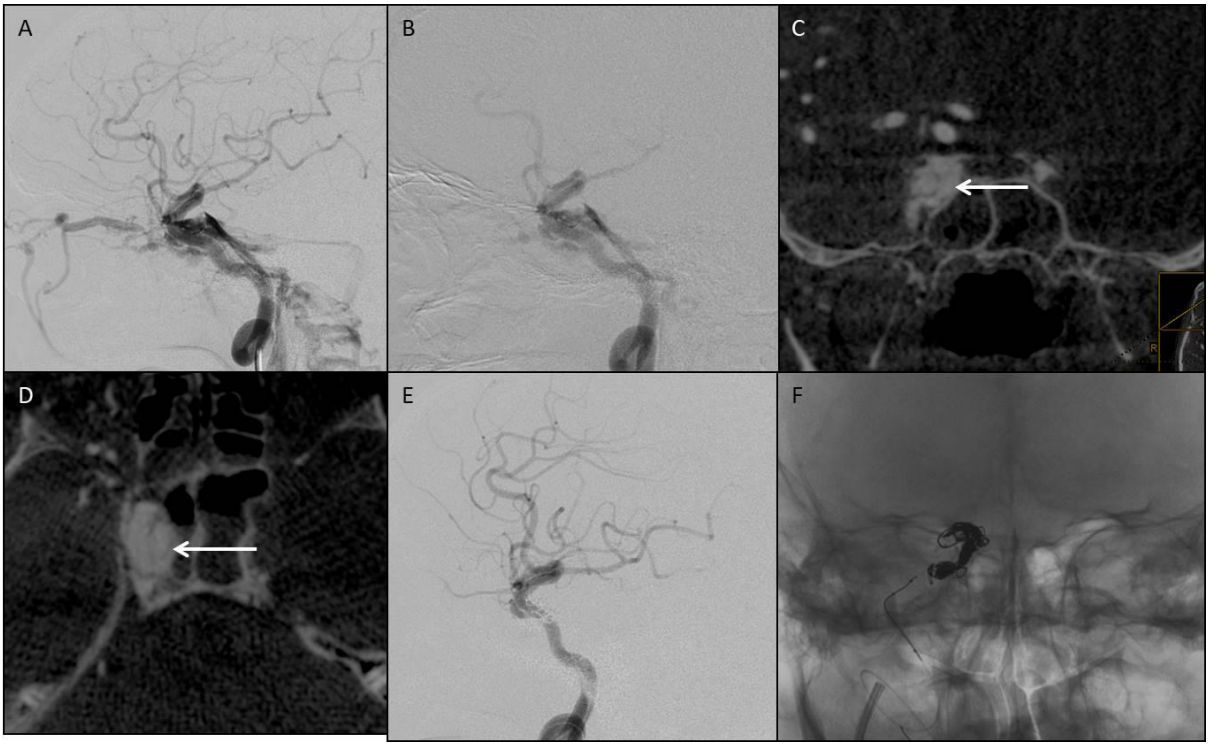

Fig 8: Right ICA angiogram, (A) & (B) Lat views showing direct CCF with small rent anterior and posterior venous drainage. Mehringer-Hieshima manoeuvre (B) did not localize the fistula site. 3D RA coronal (C) & axial (D) shows defect along the medial aspect of the horizontal segment (white arrow). Left ICA angiogram post transarterial coil embolization (E) reveals complete obliteration of the shunt. Radiograph of the skull AP view (F) shows coil mass in the cavernous sac.

Case 9: Right direct CCF with large rent.

A 29-year-old male involved in road traffic accident sustained a head injury and facial fractures. Later developed right eye proptosis, redness, and diplopia. DSA revealed right direct CCF. Underwent PAO.

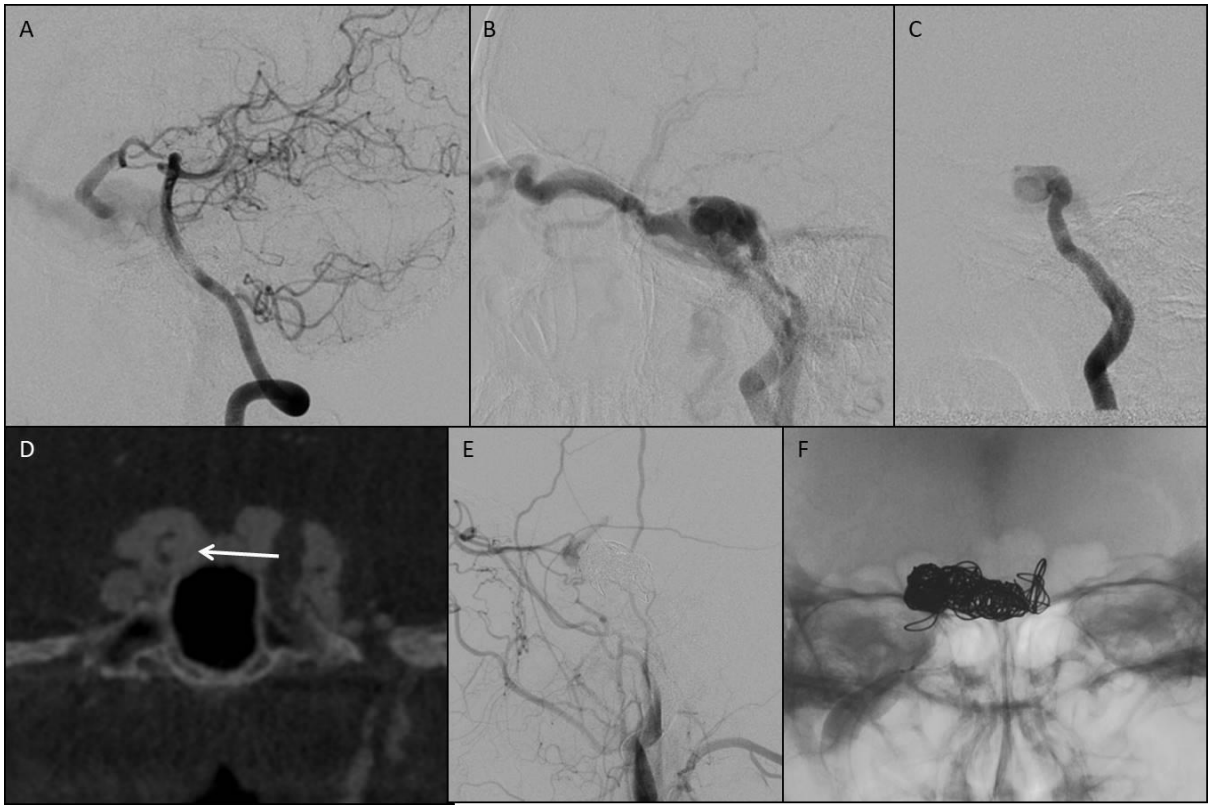

Fig 9: Right VA angiogram, Heuber manoeuvre (A) shows the location of the fistula in the horizontal segment. Right ICA angiogram (B) Lat views showing direct CCF with a large rent anterior and posterior venous drainage with cortical venous reflux. Mehringer-Hieshima manoeuvre (C) showing the location of the fistula in the horizontal segment. 3D RA coronal (D) shows large defect along the medial aspect of the horizontal segment (white arrow). Right ICA angiogram post-PAO (E) reveals complete obliteration of the shunt stasis of flow in the right ICA. Radiograph of the skull AP view (F) shows coil mass in the cavernous sac.

Case 10: Left Direct CCF, failed balloon embolization managed with coiling

A 34-year-old male involved in RTA and sustained head injury. After few days developed swelling, redness and proptosis of the left eye, and diplopia. DSA revealed left direct CCF. Balloon embolization attempted but failed due to the migration of the balloon and later underwent transarterial coiling.

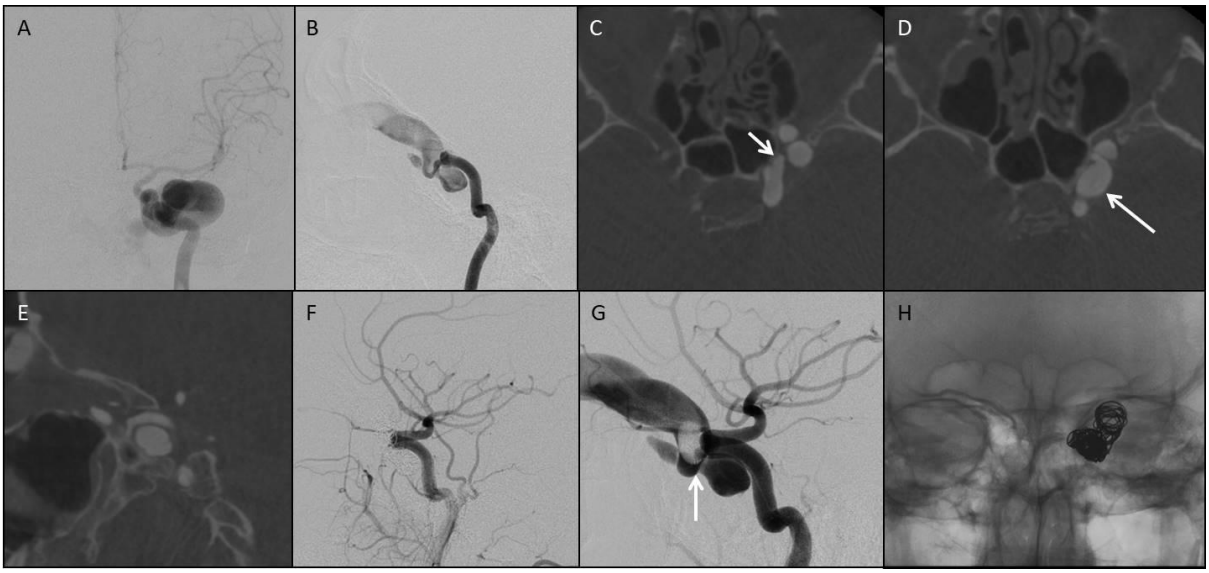

Fig 10: Left ICA angiogram (A) and (B) AP and lateral view show direct CCF with small rent. Mehringer-Hieshima manoeuvre (B) reveals a small rent in the anterior genu with a cavernous sac. 3D RA Axial (C) (D) & (E) shows a small defect with small primary sac leading to a larger secondary sac (white arrow). Left ICA angiogram (G) reveals an inflated balloon in the SOV with persistent fistula. Left ICA angiogram post transarterial coiling (F) shows complete obliteration of the shunt. Radiograph of the skull AP view (F) shows coil mass in the cavernous sac.

Discussion

7.1 Demographics & Clinical features

The predominant distribution of the cases (68%) was between the age of 21 to 40 years, and the most common presentation was with ocular/orbital symptoms in our cohort. Though the majority of the patients had anterior drainage related to the side of the fistula, bilateral and contralateral symptoms were also observed. An aggressive presentation such as intracranial bleed was noted in 2 % (One). The demographic and clinical presentation was similar to the reported studies in the literature (4,5,20).

Skull base fracture was associated with CCF in half of our patient population. The overall incidence of CCF in skull base fractures is 3.8% (12), and skull base fracture is seen in up to 32 % of the traumatic CCF (12). In traumatic CCF the rupture of the artery is not only due to tear of the artery by the bone fragment, but it can also be caused by the shearing force acting on the vessel wall or increased intraluminal pressure from distal compression of the vessel leading to the fistula (22).

7.2 Angiographic characteristics:

The effect of successful endovascular treatment in traumatic CCF is dramatic with rapid recovery of the symptoms. The treatment goal is the exclusion of the fistula with preservation of the ICA. This has to be achieved without periprocedural complication, treatment failure, and recurrence.

DB was the preferred embolic agents across many centers; however, its use has reduced due to non-availability and issues like premature detachment, retraction or migration into the ICA, or ICA compromise (4,20,57). DB is relatively inexpensive and simple to use and have an advantage of being flow guided, alternate inflation and deflation of the balloon helps in the understanding of the anatomy and dynamics of the fistula, and also provide a

possibility of repeated repositioning (6,10). The balloons have a failure rate of 5 – 10% in the literature which is attributed to an inability to navigate the balloon through the fistula or inability to achieve a complete cessation of the flow without compromising the ICA lumen(2,6,8,15). Larger fistula and shallow cavernous sac predispose to balloon migration, embolization or protrusion into the ICA lumen(58).

Transarterial coiling is being performed by most of the centers now. The advantage of coil embolization is retrievability, repositioning and availability are various sizes. The disadvantage being cost, coil migration or prolapse and mass effect causing cranial nerve palsy(25).

The endovascular stent graft can be considered for failed or recurrent cases initially treated with detachable balloons of coils or as an alternative when these options are not feasible (10). The main disadvantage is the stiff profile of the device making the navigability difficult in a tortuous ICA and also increase the risk for dissection and spasm (10,53,54).

Flow diverters have been used as an adjuvant to balloons or coils or solely with telescoping of multiple devices. The drawbacks are cost, and of long-term antiplatelets use (3). Parent vessel occlusion (PAO) is an alternative option done in difficult, failed or recurrent cases, either endovascular or surgically (2).

In our series 64% underwent the constructive procedure with the maintenance of the ICA patency. DB embolization was performed in 55%, detachable coils in 41% and covered stent in 3% (one case). 35% underwent endovascular trapping of fistula or PAO. The success rate of DB in excluding the fistula with preservation of the parent artery was 61.5 %. The rate of parent artery sacrifice, recurrence rate and failure rate for DB were 23%, 15%, and 27% respectively. The success rate of coils in fistula closure was 100% with no recurrence. In the study of 172 cases of traumatic CCF by Chin CT et al. the rate of successful endovascular fistula occlusion was 94%. The rate of successful fistula occlusion with preservation of the

carotid artery was 70% (7). Lin CT et al. in their study had a successful fistula occlusion rate of 71 % with a recurrence rate of 28 % and failure rate of 20% (12).

The various factors that need to be considered prior to intervention include the size of rent, the extent of arterial involvement, size of the cavernous sinus, and the status of collateral circulation (REF). It is also essential to know the relation and orientation of the cavernous sac to the fistula. Chi CT et al. have noted that the incidence of the requirement for PAO is significantly higher in cases with large fistula and the incidence of balloon failure is higher with the small fistulas (7).

In our study, 3D RA allowed for precise analysis of the CCF including the size, number, and location of the rents and the size of the first cavernous sac in all 44 cases. For this purpose, 2D DSA required additional maneuvers, despite which the measurement of the fistula size was not possible in 28% of the CCFs. 2D DSA either undersized or oversized the rent and the first cavernous sac in 41% and 57% of the patients respectively. If the fistula were imaged in profile on the lateral projection in 2D DSA and was either small or medium-sized their measurement matched accurately with that of 3D RA. Thus the reason for under sizing of the rent is probably the speed of the shunt and the direction of the fistula flow which could partly be overcome by use of compression maneuvers and oblique projection which is not always feasible. A comparative study in intracranial aneurysms has shown the 2D DSA undersized 73% of the aneurysms as compared to 3D DSA, in particular, smaller aneurysms (< 5 mm)(47).

The analysis of the fistula on 2D DSA is based on looking for the first appearance of the contrast outside the confines of the artery. The problem in making this assessment on the 2D image is the superimposition of the normal vascular outline over the presumed site of fistula, rapid opacification of the adjacent cavernous sac obscuring the fistulous site and high flow nature of the fistula. 3D RA provides an opportunity to view the fistula in multiple

planes and various projections. The relation of the fistula to the cavernous sac and the ratio of their sizes can also be estimated on 3D RA.

In our study, the false localization of the fistula on 2D DSA was seen in 30 to 50% cases with the higher number of discordant fistulas located in the posterior vertical segment and posterior genu. The identification of exact location helps in cannulation, might predict the success of balloon as distal location and tortuous arteries might preclude successful cannulation.

3D RA also gives a cross-sectional view of the artery at the site of the fistula which provides certain additional information like the caliber and configuration of the artery and location of the rent on the arterial wall. The information on the configuration of the artery like dilatation of the artery or flattening of the artery at the site of the rent is helpful in choosing the hardware as in, the size of the balloon or stent if assisted coiling is planned or choosing the most appropriate treatment. In our study, we did notice that most of the cases with large size fistula had flattening of the artery at the site of the rent. The identification of the location of the defect on the anterior, posterior, medial and lateral wall also improves the confidence of the operator in cannulating the rent during embolization (image). 3D RA can also be used to obtain a working angle to separate the venous pouch from the ICA for intervention. This is akin to precise identification of the neck of an aneurysm and getting the appropriate working angle for intervention for which 3D RA is superior to 2D DSA(59,60).

Comparison studies done in intracranial aneurysms have shown that 3D DSA is valuable in performing accurate measurement and finding the working view and is a supplement to 2D DSA in planning endovascular treatment (59). The size of an aneurysm and the diameter of the neck are accurately measured on 3D DSA (13,61).

CTA and MDCT with near isotropic data set and good spatial resolution have also been used for identification of the fistula. Chen CCC et al. retrospectively evaluated 53

patients with direct CCF and found that CTA was as useful as 2D DSA in the determination of the location of the fistula(36). Lee JY et al. studied eight cases of direct CCF using MDCT in whom the fistula was detected by identifying the dehiscent ICA wall. MDCT showed a sensitivity of 100% and specificity of 75-88% in identification of the fistulous site. Also, it provided information on the size and direction of the fistula and venous pouch(37). The disadvantage of MDCT is there is opacification of all the vessels as it is performed with transvenous injection unlike selective arterial injection in 3D RA and hence delineation of the artery from vein could be difficult in high flow situations. Most importantly the spatial resolution is inferior to 3D RA(62).

The assessment on 2D has much subjectivity to it and is not precise, unlike the 3D DSA which is explained by the fair interreader agreement for 2D DSA compared to moderate for 3D DSA in the evaluation of the fistula. In our study, the evaluation on 3D RA significantly improved the confidence of the readers in the assessment of the fistula ($p < 0.001$) be it size, number, and location as compared to 2D DSA.

Kwon BJ studied the usefulness of 3D RA in endovascular occlusion of the CCF with a detachable balloon. They performed both 2D DSA and 3D RA in pretreatment, post-balloon inflation-pre-detachment and post-detachment stage of 5 patients. They found 3D to be useful in assessing the complex perifistular anatomy in the pretreatment stage and provide information on the location and extent of inflation of the balloon, the presence of pseudoaneurysm and traction induced instability in the pre-detachment stage(50).

It is possible that with the performance of 3D RA the compression maneuvers (Heuber and Mehringer-Hieshima) can be skipped from the standard angiographic protocol for CCF patients which in turn would reduce the procedure time, contrast dose used and radiation dose. We did not evaluate this in our study; however similar comparative studies in

intracranial aneurysms have shown that 3D DSA detected more aneurysms with a significant reduction in the radiation dose, contrast volume and procedural time(61,63).

The other additional advantages of 3D RA include, due to its ability of reformation in multiple planes and its significantly improved resolution, it is helpful to pick additional associated finding like dissection, pseudoaneurysm, and arterial transection. There were six (pseudoaneurysm, n = 3; transection, n = 1; dissection, n = 1, ectasia/dysplasia, n = 1) such instances in our study which were missed on 2D DSA. One case with medially directed sac eroding into the sphenoid sinus was also picked by 3D RA.

7.3 Therapeutic decision:

In our study, the agreement between the actual treatment and the treatment choice based on combined 2D DSA and 3D RA improved over that of 2D DSA alone. This improvement was irrespective of the experience of the reviewers. However, the level of agreement was not very high, mainly for the choice of destructive option. The reason is that other factors like balloon failure, recurrence after balloon embolization and presence of additional findings (pseudoaneurysms and vessel dysplasia) influenced the final treatment of PAO in these cases.

There was a better inter-reader agreement for treatment choice made on combined 2D DSA and 3D RA (Kappa: 0.585) as compared to 2D DSA alone (Kappa: 0. 100).

Similarly, the agreement between the actual treatment and the preferred embolic agent on combined 3D RA and 2D DSA improved over that of the 2D DSA. This improvement was irrespective of the experience of the reviewers. Though the interreeder agreement improved for the choice of the preferred embolic agent with 2D DSA when combined with 3D RA, the agreement was only fair. This low level of agreement is possibly due to the difference in the level of experience between the readers. The experienced reader is equipped with his past

experiences and previous failure with the embolic agent and the knowledge of institution treatment protocols, which would have influenced his choice as compared to the inexperienced reviewer.

Our analysis of the CCF with 2D DSA, when combined with 3D RA significantly, improved the quality of assessment and added confidence in the decision on the choice of treatment and embolic agent ($p < 0.001$).

Though there are no similar studies in CCF, studies in intracranial aneurysms have shown that 3D RA is useful in planning surgery and endovascular therapy(13,46,64). The 3D data reproduces the vascular anatomy and its relations and helps neurosurgeon to anticipate the difficulties during surgical access and clipping of the aneurysms(46).

7.4 Subclassification:

The incidence of treatment failure particularly with detachable balloons is 5 – 10% in the literature(2,6,8,15). One of the cause of treatment failure with a detachable balloon is due to its inability to be navigated through the fistula. In our study, there were 6 cases of balloon failures. Among the failure cases, three patients had a small-sized fistula, and the failure was due to difficulty in navigating the balloon into the cavernous sac in two. In one the failure was due to the migration of the balloon into the SOV as the patient, also, had a very small venous sac. Three other cases had a large fistula, and the failure was due to the inadequate cessation of the flow on balloon inflation in two and ICA narrowing in one. Four cases of balloon failure got converted to PAO among them three had large rent, and one had small rent.

Multiple endovascular treatments could increase the risk of complication and overall expense of the treatment. Thus anticipation of the preferred embolic agent before the procedure is helpful especially in a developing country with scarce resources. It would also

help in appropriate counseling of the patient prior to the intervention. As the accurate estimation of the size of the rent on 2D DSA is not possible, indirect estimation of the size is performed by looking at the extent of steal across the fistula (partial or complete). Partial steal is seen in small and medium fistula; the small-sized fistula shows antegrade flow in both ACA and MCA while medium-size fistula is showing it in either. The large fistula shows complete steal. Studies have shown that this method of subclassification has been useful(65,66). This classification does not consider individual differences in ACOM development/hypoplasia. Another issue would be a wrongful classification especially if angiogram is performed under general anesthesia. The reduced intracranial tension caused by the anaesthetic agent could potentially influence the grading of the fistula.

In our study, we classified the rent based on the sector of arterial involvement and found that the choice of treatment could be reliably predicted based on the sectorial cut off of 90º. On dichotomisation of the sectorial angle into < 90° and >90° it is seen that 76% of the cases with angle less than 90º received constructive management whereas equal number of CCFs in the group above 90º received constructive or destructive management. In the group with angle less than 90º equal number of patients were treated with balloon or coils whereas in the group above 90º majority (70%) were treated with DB. Further we attempted to measure the angle of the defect in each artery and these were correlated with the actual treatment. The observations largely matched the hypothetical classification. It was noted that 75% of the CCFs who underwent constructive treatment had an angle of defect below 100° and 75% of the CCFs treated with destructive treatment like PAO had an angle of defect above 100° ($p < 0.001$). In our study 75% of the cases with an angle of defect between 60° to 100° were treated with DB. Transarterial coiling was done when the angle of defect was between 40° to 90° in 75% of the cases and this choice was primarily due to the inability of navigation of the DB across a small rent or small size of the primary sac.

Our study shows that identifying the extent of involvement have a predictive role in choosing an appropriate treatment in a given CCF. It is conceivable that smaller rent permits constructive treatment without compromising the arterial lumen in case of detachable balloon or favours coiling without the need for adjunctive methods such as stents. 3D RA could identify the extent of embolic device that could be exposed into the arterial lumen and hence the treatment options could be decided accordingly. However, this classification is relevant only when detachable balloons or primary coiling vs destructive methods are considered as therapeutic options. Theoretically, constructive techniques could be done in most of the situations, using stents, covered grafts or flow diverters, however, these options could increase the overall cost of the procedure, may need antiplatelet therapy which could hamper progressive occlusion in residual fistula. (67)

In our study 55% of the fistula classified as small on 2D DSA were treated with coils and incidence of PAO was 6%. Almost equal number of cases in the medium-sized fistula group were treated with balloons and coils. The incidence of PAO in medium size group was 12% and in the large size group was 70%. Chi CT et al. in their study had an ICA occlusion rate of 18% for medium and 53.9% for large fistulas. They treated most of the small fistula with coils as they had balloon failure in the initial 9 cases in their cohort. The preferred embolic agent for medium-sized fistula in their study was balloons or sometime balloon with coils when one is not sufficient.

Limitations: The limitations of our study were a small sample size and limited availability of embolic material. Due to financial constrain, the institution treatment protocol was favoured to procedure and devices with low cost and also balloon first approach was followed which explains a slightly higher failure and recurrence rate.

Conclusion

In the assessment of traumatic CCF, our study showed that:

- 3D RA allowed for precise analysis of the CCF including the size, number and location of the rents, the size of the first cavernous sac and significantly improved the confidence of the reviewer in making this assessment.
- The treatment choice made and embolic agent chosen based on combined 2D DSA and 3D RA agreed better with the actual treatment than that of 2D DSA alone. This was irrespective of the experience of the reviewer.
- 2D DSA, when combined with 3D RA significantly, improved the quality of assessment and added confidence in the decision on the choice of treatment and embolic agent.
- Measuring the sector of defect may be helpful in choosing the treatment

References:

1. Min L, Ghaith H, Jeffrey P M, Peter A R. A brief history of carotid-cavernous fistula. J Neurosurg. 2016;126(June):1–7.

2. Korkmazer B, Kocak B, Tureci E, Islak C, Kocer N, Kizilkilic O. Endovascular treatment of carotid cavernous sinus fistula: A systematic review. World J Radiol [Internet]. 2013;5(4):143–55.

3. Nadarajah M, Power M, Barry B, Wenderoth J. Treatment of a traumatic carotid-cavernous fistula by the sole use of a flow diverting stent. J Neurointerv Surg. 2012;4:e1–e1.

4. Gupta AK, Purkayastha S, Krishnamoorthy T, Bodhey NK, Kapilamoorthy TR, Kesavadas C, et al. Endovascular treatment of direct carotid cavernous fistulae: A pictorial review. Neuroradiology. 2006;48(11):831–9.

5. Wang W, Li YD, Li MH, Tan HQ, Gu BX, Wang J, et al. Endovascular treatment of post-traumatic direct carotid-cavernous fistulas: A single-center experience. J Clin Neurosci [Internet]. 2011;18(1):24–8.

6. Lu X, Hussain M, Ni L, Huang Q. A comparison of different transarterial embolization techniques for direct carotid cavernous fistulas : a single center experience in 32 patients. J Vasc Interv Neurol. 2014;7(5):35–47.

7. Chi CT, Nguyen D, Duc VT, Chau HH, Son VT. Direct Traumatic Carotid Cavernous Fistula: Angiographic Classification and Treatment Strategies Study of 172 Cases. Interv Neuroradiol [Internet]. 2014 Jul;20(4):461–75.

8. Xu XQ, Liu S, Zu QQ, Zhao LB, Xia JG, Zhou CG, et al. Follow-up of 58 traumatic carotid-cavernous fistulas after endovascular detachable-balloon embolization at a single center. J Clin Neurol. 2013;9(2):83–90.

9. Luo CB, Teng MMH, Chang FC, Lin CJ, Guo WY, Chang CY. Transarterial detachable coil embolization of direct carotid-cavernous fistula: Immediate and long-term outcomes. J Chinese Med Assoc [Internet]. 2013;76(1):31–6.

10. Archondakis E, Pero G, Valvassori L, Boccardi E, Scialfa G. Angiographic follow-up of traumatic carotid cavernous fistulas treated with endovascular stent graft placement. Am J Neuroradiol. 2007;28(2):342–7.

11. Li J, Lan ZG, Xie XD, You C, He M. Traumatic carotid-cavernous fistulas treated with covered stents: Experience of 12 cases. World Neurosurg [Internet]. 2010;73(5):514–9.

12. Lin TC, Mao SH, Chen CH, Chen YL, Wong HF, Chang CJ, et al. Systematic Analysis of the Risk Factors Affecting the Recurrence of Traumatic Carotid-Cavernous Sinus Fistula. World Neurosurg. 2016;90:539–545.E1.

13. Hochmuth A, Spetzger U, Schumacher M. Comparison of three-dimensional rotational angiography with digital subtraction angiography in the assessment of ruptured cerebral aneurysms. AJNR Am J Neuroradiol [Internet]. 2002;23(7):1199–205.

14. Serafin Z, Strzeaśniewski P, Lasek W, Beuth W. Follow-up after embolization of

ruptured intracranial aneurysms: A prospective comparison of two-dimensional digital subtraction angiography, three-dimensional digital subtraction angiography, and time-of-flight magnetic resonance angiography. Neuroradiology. 2012;54(11):1253–60.

15. Naesens R, Mestdagh C, Breemersch M, Defreyne L. Direct Carotid-Cavernous Fistula : a Case Report and Review of the Literature. Bull Soc belge Ophtalmol. 2006;43–54.

16. Ogilvy CS, Motiei-Langroudi R, Ghorbani M, Griessenauer CJ, Alturki AY, Thomas AJ. Flow Diverters as Useful Adjunct to Traditional Endovascular Techniques in Treatment of Direct Carotid-Cavernous Fistulas. World Neurosurg [Internet]. 2017;105:812–7.

17. Benndorf G, SpringerLink (Online service). Dural Cavernous Sinus Fistulas Diagnostic and Endovascular Therapy [Internet]. A. L. Baert L, M. Knauth, Göttingen K. Sartor H, editors. Springer-Verlag Berlin Heidelberg; 2010.

18. Gemmete JJ, Ansari SA, Gandhi DM. Endovascular techniques for treatment of carotid-cavernous fistula. J neuro-ophthalmology [Internet]. 2009;29(1):62–71.

19. Ducruet AF, Albuquerque FC, Crowley RW, McDougall CG. The evolution of endovascular treatment of carotid cavernous fistulas: A single-center experience. World Neurosurg [Internet]. 2013;80(5):538–48.

20. Lewis AI, Tomsick TA, Tew Jr. JM, Standard SC, Chavis TD, Hopkins LN, et al. Management of 100 consecutive direct carotid-cavernous fistulas: Results of treatment with detachable balloons. Neurosurgery [Internet]. 1995;36(2):239–45.

21. Baugnon KL, Hudgins PA. Skull base fractures and their complications. Neuroimaging Clin N Am [Internet]. 2014;24(3):439–65.

22. Ellis JA, Goldstein H, Connolly ES, Meyers PM. Carotid-cavernous fistulas. Neurosurg Focus [Internet]. 2012 May;32(5):E9.

23. Gemmete JJ, Ansari SA, Gandhi D. Endovascular Treatment of Carotid Cavernous Fistulas. Neuroimaging Clin N Am [Internet]. 2009;19(2):241–55.

24. Zanaty M, Chalouhi N, Tjoumakaris SI, Hasan D, Rosenwasser RH, Jabbour P. Endovascular treatment of carotid-cavernous fistulas. Neurosurg Clin N Am [Internet]. 2014;25(3):551–63.

25. Yu Y, Li Q, Huang Q, Zhang Y, Fang Y, Xu Y, et al. Embolization of direct carotid cavernous fistula with Onyx and coils under transarterial balloon protection. Cardiovasc Intervent Radiol. 2014;37(3):679–85.

26. Talks SJ, Salmon JF, Elston JS, Bron AJ. Cavernous-dural Fistula With Secondary Angle-closure Glaucoma. Am J Ophthalmol [Internet]. 1997 Dec;124(6):851–3.

27. Chaudhry I a, Elkhamry SM, Al-Rashed W, Bosley TM. Carotid cavernous fistula: ophthalmological implications. Middle East Afr J Ophthalmol [Internet]. 2009;16(2):57–63.

28. Miller NR. Diagnosis and management of dural carotid-cavernous sinus fistulas. Neurosurg Focus. 2007;23(5):E13: 1-15.

29. Das S, Bendok BR, Novakovic RL, Parkinson RJ, Rosengart AJ, Macdonald RL, et al. Return of vision after transarterial coiling of a carotid cavernous sinus fistula: case report. Surg Neurol. 2006;66(1):82–5.

30. Albuquerque FC, Heinz GW, McDougall CG. Reversal Of Blindness After Transvenous Embolization Of A Carotid-Cavernous Fistula: Case Report. Neurosurgery. 2003;52(1):233–7.

31. Halbach V V, Hieshima G, Higashida BR, Reicher TM. Carotid Cavernous Fistulae: Indications for Urgent Treatment. Am J Roentgenol. 1987;

32. Hayashi K, Suyama K, Nagata I. Traumatic carotid cavernous fistula complicated with intracerebral hemorrhage: case report. Neurol Med Chir (Tokyo) [Internet]. 2011;51(3):214–6.

33. Yu J, Guo Y, Zhao S, Xu K. Brainstem edema caused by traumatic carotid-cavernous fistula: A case report and review of the literature. Exp Ther Med. 2015;10(2):445–50.

34. Wyrick D, Smith SD, Dassinger MS. Traumatic carotid-cavernous fistula presenting as massive epistaxis. J Pediatr Surg [Internet]. 2013;48(4):883–6.

35. Baccin C., Campos CM., Abicalaf R, Kanashiro LH., Bolcato M., Lima S., et al. Traumatic Carotid-Cavernous Fistula : Endovascular Treatment with Onyx and Coils. Interv Neuroradiol [Internet]. 2005 Dec 22;1996(4):363–7.

36. Chen CC-C, Chang PC-T, Shy C-G, Chen W-S, Hung H-C. CT angiography and MR angiography in the evaluation of carotid cavernous sinus fistula prior to embolization: a comparison of techniques. Am J Neuroradiol. 2005;26(9):2349–56.

37. Lee JY, Jung C, Ihn YK, Kim DJ, Seong SO, Kwon BJ. Multidetector CT angiography in the diagnosis and classification of carotid-cavernous fistula. Clin Radiol. 2016;71(1):e64–71.

38. Duan Y, Liu X, Zhou X, Cao T, Ruan L, Zhao Y. Diagnosis and follow-up study of carotid cavernous fistulas with color Doppler ultrasonography: analysis of 33 cases. J Ultrasound Med [Internet]. 2005 Jun;24(6):739–45.

39. Chen YW, Jeng JS, Liu HM, Hwang BS, Lin WH, Yip PK. Carotid and transcranial color-coded duplex sonography in different types of carotid-cavernous fistula. Stroke. 2000;31(3):701–6.

40. Mehringer CM, Hieshima GB, Grinnell VS, Tsai F, Pribram HF. Improved localization of carotid cavernous fistula during angiography. Am J Neuroradiol. 1982;3(1):82–4.

41. Rajagopal R, Mehta N, Saran S, Khera PS. Heuber Maneuver in Evaluation of Direct Carotid-Cavernous Fistula. Polish J Radiol [Internet]. 2016;81:483–5.

42. Szkup P, Beningfield S. Endovascular treatment of post-traumatic carotid-cavernous fistulae using latex detachable balloons. South African J Radiol [Internet]. 2005 Jan 4;9(1).

43. Samaniego E a., Martinez-Galdamez M, Abdo G. Treatment of direct carotid-cavernous fistulas with a double lumen balloon. J Neurointerv Surg [Internet]. 2015;1–5.

44. Sorteberg A. Balloon occlusion tests and therapeutic vessel occlusions revisited: When, when not, and how. Am J Neuroradiol. 2014;39(5):862–5.

45. Moret J, Kemkers R, Op de Beek J, Koppe R, Klotz E, Grass M. 3D-Rotational Angriography: Clinical value in endovascular treatment. Med mundi. 1998;42(3):8–14.

46. Thines L, Taschner C, Lejeune J-P, Le Thuc V, Pruvo J-P, Bourgeois P, et al. Surgical views from three-dimensional digital subtraction angiography for the planning of aneurysm surgery. J Neuroradiol. 2007;34(3):205–11.

47. Kawashima M, Kitahara T, Soma K, Fujii K. Three-dimensional digital subtraction angiography vs two-dimensional digital subtraction angiography for detection of ruptured intracranial aneurysms: a study of 86 aneurysms. Neurol India [Internet]. 2005;53(3):287–9; discussion 290.

48. Kumar S, Gaikwad SB, Mishra NK. 3D Rotational Angiography in Follow-Up of Clipped Intracranial Aneurysms. ISRN Radiol [Internet]. 2014;2014:1–5.

49. Varadharajan S, Ramalingaiah AH, Saini J, Gupta AK, Das S. Order Among Chaos—Value of 3-Dimensional Rotational Angiography in Direct Carotid-Cavernous Fistulas. World Neurosurg [Internet]. 2016;92:573–4.

50. Kwon BJ, Han MH, Kang HS, Chang KH. Endovascular occlusion of direct carotid cavernous fistula with detachable balloons: Usefulness of 3D angiography. Neuroradiology. 2005;47(4):271–81.

51. Yu Y, Huang Q, Xu Y, Hong B, Zhao W, Deng B, et al. Use of onyx for transarterial balloon-assisted embolization of traumatic carotid cavernous fistulas: A report of 23 cases. Am J Neuroradiol. 2012;33(7):1305–9.

52. Ramalingaiah AH, Prasad C, Sabharwal PS, Saini J, Pandey P. Transarterial treatment of direct carotico-cavernous fistulas with coils and Onyx. Neuroradiology. 2013;55(10):1213–20.

53. Wang W, Li MH, Li YD, Gu BX, Lu HT. Reconstruction of the Internal Carotid Artery after Treatment of Complex Traumatic Direct Carotid-Cavernous Fistulas with the Willis Covered Stent: A Retrospective Study with Long-Term Follow-up. Neurosurgery. 2016;79(6):794–804.

54. Tiewei Q, Ali A, Shaolei G, Feng L, Zhongsong S, Xuesong L, et al. Carotid cavernous fistulas treated by endovascular covered stent grafts with follow-up results. Br J Neurosurg [Internet]. 2010;24(4):435–40.

55. Hayashi N, Okada H, Tomura N, Sasaki T, Kuwata T. Transvenous Target Embolization for a Small Sized, Non-traumatic Direct Carotid-cavernous Fistula using a Single Coil: Technical Case Report. J Neuroendovascular Ther [Internet]. 2016;10(5):272–7.

56. Shwe Y, Paramasivam S, Ortega-Gutierrez S, Altschul D, Berenstein A, Fifi JT. High-Flow Carotid Cavernous Fistula and the Use of a Microvascular Plug System: Initial Experience. Interv Neurol [Internet]. 2014;3(2):78–84. 7

57. Langford KH, Vitek JJ, Zeiger E. Migration of detachable mini-balloon from the ICA causing occlusion of the MCA: Case report. J Neurosurg [Internet]. 1983;58(3):430–4.

58. Graeb DA, Robertson WD, Lapointe JS, Nugent RA. Avoiding intraarterial balloon detachment in the treatment of posttraumatic carotid-cavernous fistulae with detachable balloons. Am J Neuroradiol. 1985;6(4):602–5.

59. Anxionnat R, Bracard S, Ducrocq X, Trousset Y, Launay L, Kerrien E, et al. Intracranial aneurysms: clinical value of 3D digital subtraction angiography in the therapeutic decision and endovascular treatment. Radiology [Internet]. 2001;218(3):799–808.

60. Toyota S, Iwaisako K, Takimoto H, Yoshimine T. Intravenous 3D digital subtraction angiography in the diagnosis of unruptured intracranial aneurysms. AJNR Am J Neuroradiol [Internet]. 2008;29(1):107–9.

61. Wong SC, Nawawi O, Ramli N, Abd Kadir KA. Benefits of 3D Rotational DSA Compared with 2D DSA in the Evaluation of Intracranial Aneurysm. Acad Radiol. 2012;19(6):701–7.

62. Lu L, Zhang LJ, Poon CS, Wu SY, Zhou CS, Luo S, et al. Digital Subtraction CT Angiography for Detection of Intracranial Aneurysms: Comparison with Three-dimensional Digital Subtraction Angiography. Radiology [Internet]. 2012;262(2):605–12.

63. Tonkopi E, Al-Habsi AH, Shankar JJ. Radiation Dose from 3D Rotational vs. Conventional 2D Digital Subtraction Angiography in Intracranial Aneurysm Coiling. Can J Neurol Sci [Internet]. 2015;42(3):176–80.

64. Missler U, Hundt C, Wiesmann M, Mayer T, Brückmann H. Three-dimensional reconstructed rotational digital subtraction angiography in planning treatment of intracranial aneurysms. Eur Radiol. 2000;10(4):564–8.

65. Son VT an. Direct traumatic carotid cavernous fistula: angiographic classification and treatment strategies. Study of 172 cases. Interv Neuroradiol. 2014;20(4):461–75.

66. Malan J, Lefeuvre D, Mngomezulu V, Taylor A. Angioarchitecture and treatment modalities in posttraumatic carotid cavernous fistulae. Interv Neuroradiol. 2012;18(2):178–86.

67. La Tessa G, Pasqualetto L, Catalano G, Marino M, Gargano C, Cirillo L, et al. Traumatic carotid cavernous fistula: failure of endovascular treatment with two stent-grafts. Interv Neuroradiol [Internet]. 2005;11(4):369–75.

CONSENT FORM (Annexure 1)

TITLE OF THE STUDY: - COMPARISON OF 3D ROTATIONAL ANGIOGRAPHY WITH DIGITAL SUBTRACTION ANGIOGRAPHY IN SUB CLASSIFICATION AND TREATMENT PLANNING OF DIRECT CAROTID CAVERNOUS FISTULA.

You …… have been informed that you have abnormal connections between blood vessels (arteries and veins) in the coverings of brain in the region of cavernous sinus (blood containing sac in the middle of skull base). If the condition is left untreated it may cause permanent loss of vision and sometimes hemorrhage in brain. You are required to undergo a special X-ray examination Arteriogram/DSA Digital sub-subtraction Angiogram to know the size, shape and extent of these blood vessels. You are being requested to participate in a study which will compare 3D rotational angiography with digital subtraction angiography in sub classification and treatment planning of direct carotid cavernous fistula (same disease as yours). For this purpose, the data from your clinical records, investigations, endovascular treatment procedures and follow up investigations will be accessed and analyzed.

The other treatment option available to you is Surgery. Since it is difficult to operate, there is an alternate way of treating these unnecessary blood vessel connections by permanently blocking these blood vessels. For this a long tube is inserted into the blood vessels in your groin and negotiated close the area of the abnormal blood vessels, while watching its progress on the Television screen. After confirming the position of the tube in its proper place, small balloon/balloons are intentionally detached or metal coils delivered through the tube which will instantly block the blood vessels or abnormal connection. This procedure is performed under general anesthesia. This may take sometimes 3 to 4 hours after which anesthesia will be reversed. If this treatment is complete, repeat procedure may not be required. On the other hand repeat procedure might be required if complete blocking was not possible.

Though the above method has been oversimplified, it is complicated and is associated with certain risks. In the groin the blood vessel may be obstructed due to clot formation requiring minor operation to save the leg. If the balloon or tube are beyond control and lodge in any other area, normal areas of brain may suffer from poor blood supply. This may result in either temporary or permanent paralysis, loss of speech, loss of vision or loss of memory. Rarely a state of unconsciousness (coma) or even death may occur. Best of efforts will be exercised towards treatment while avoiding such complications. We attempt to make you aware that this is a very special procedure carrying very small but significant risks and it is performed only because this is the only alternative or pre-operative measure. If you like any more detailed information, we will be glad to discuss further with you.

Does this study pose any side effects to the participant?

NO. We will be accessing the angiographic details of an endovascular procedure and assess the effect of addition of 3D rotational angiography (which is an already established standard of care at this institute) which will be performed on you.

If you take part what will you have to do?

If you agree to participate in this study, you will be required to come to the hospital 3 months after the surgical procedure, this will coincide with your normal treatment routine, so that you don't have to come to the hospital exclusively for this study. All other treatments that you are already on will be continued and your regular treatment will not be changed during this study. No additional procedures or blood tests will be conducted routinely for this study. If at any time you experience any problems, you will be expected to report this to the doctor.

Can you withdraw from this study after it starts?

Your participation in this study is entirely voluntary and you are also free to decide to withdraw permission to participate in this study. If you do so, this will not affect your usual treatment at this hospital in any way.

What will happen if you develop any study related injury?

There are **NO** additional study related injury as we are only collecting and analyzing the data from your medical records.

What happens after the study is over?
You may or may not benefit from the study, after the study we will be able to assess the effect of addition of 3D rotational angiography in sub classification and treatment planning of direct carotid cavernous fistula.

Will your personal details be kept confidential?
The results of this study will be published in a medical journal but you will not be identified by name in any publication or presentation of results. However, your medical notes may be reviewed by people associated with the study, without your additional permission, should you decide to participate in this study.

If you have any further questions you can contact me in interventional Radiology OPD or in the telephone number 04712524518, 9447961100 or email: savithkumar@sctimst.ac.in.

Signature (or Thumb impression) of the Subject/Legally Acceptable

Representative:_____ Date: _____/_____/_____

Signatory's Name: _____

Signature of the Investigator: _____Date: _____/_____/_____

Study Investigator's Name: _____

Signature of the witness (if needed) _____Date:_____/_____/_____

Name of the Witness (if needed): _____

Participant's name: Date of Birth / Age (in years):

I_____,

Son/daughter of _____

(Please tick boxes)

- Declare that I have read the above information provide to me regarding the study: Comparison of 3D rotational angiography with digital subtraction angiography in sub classification and treatment planning of direct carotid cavernous fistula and have clarified any doubts that I had. [ ]
- I also understand that my participation in this study is entirely voluntary and that I am free to withdraw permission to continue to participate at any time without affecting my usual treatment or my legal rights. [ ]

- I understand that the study staff and institutional ethics committee members will not need my permission to look at my health records even if I withdraw from the trial. I agree to this access. [ ]
- I understand that my identity will not be revealed in any information released to third parties or published. [ ]
- I voluntarily agree to take part in this study. [ ]
- I received a copy of this signed consent form. [ ]

Name:

Signature:

Date:

Name of witness:

Relation to participant:

Date:

(Person Obtaining Consent): I attest that the requirements for informed consent for the medical research project described in this form have been satisfied. I have discussed the research project with the participant and explained to him or her in nontechnical terms all of the information contained in this informed consent form. I further certify that I encouraged the participant to ask questions and that all questions asked were answered.

_____

Name and Signature of Person Obtaining Consent

Principal Investigator.

PROFORMA (Annexure 2)

Title: Comparison of 3D Rotational Angiography with Digital Subtraction Angiography in sub classification and Treatment planning of Direct Carotid Cavernous Fistula.

Anonymized patient key :

CLINICAL:

Age:

Sex:

Chief complaints/duration of symptoms:

History of presenting complaints:

Past history/treatment history:

Examination :

General examination:

System examination:
CVS Respiratory GIT/GUT CNS

Other /Local examination:

IMAGING REVIEW

USG-
CT/CT ANGIO:
MRI/MRA:

DSA (ANGIOGRAPHIC DETAILS):

- Interventional route : Transarterial/transfemoral.
- Flow in ipsilateral ACA and MCA : Present in both
  Present in either: (ACA/MCA)
  Present in neither.
- Size of defect : Small/medium/large
- Location of the defect.
- Size of cavernous sinus sac
- Venous drainage involved : Anterior
- Posterior
- Cortical venous reflux : Present/absent
- Collateral supply : ACom/PCom
- Cross compression study :
- Circulation time. :
- **Venous delay**

Quality of detection of the

Location of rent	1- good; 2- sufficient and 3- insufficient.
number of rent	1- good; 2- sufficient and 3- insufficient.
size of the rent	1- good; 2- sufficient and 3- insufficient.
Sub classification	1- good; 2- sufficient and 3- insufficient.

- **EMBOLISATION DETAILS:**
- Interventional procedure : Parent artery occlusion/ Reconstructive
- Agent used : Balloon / Coil
- Size of balloon used :
- Number of balloon or coils used:
- Supplemental embolic agent used:
- Procedure duration

- Angiographic result : Complete/incomplete
- Hardware used.

  Guiding sheath
  Angio catheter
  Micro catheters
  Micro wires
- Complications / technical difficulties if any
- Heparin Dose
- Reversal if any required

Therapeutic decision

What is the first option of treatment? (Constructive or destructive)
Quality of choice of response 1- good; 2- sufficient and 3- insufficient.
Which is the preferred embolic agent? (balloon, coil, stent or liquid agents) ;
Quality of choice of response 1- good; 2- sufficient and 3- insufficient.

FOLLOW UP CLINICAL

Immediate post procedure - Relief from symptoms
Stability of result at 3 months
Persisting symptoms if any
Improvement/worsening if any
New symptoms if any

Definition:

Location of rent (define the segments of the cavernous sinus) 1- good; 2- sufficient and 3- insufficient.
Good = accurately able to locate the rent.
Sufficient = Able to locate the probably site of rent how ever not very confident
Insufficient = Not able to locate the rent

Number of rent (single or multiple) 1- good; 2- sufficient and 3- insufficient.
Good = able to say single or multiple .
Sufficient = Able to in saying single or multiple how ever not very confident
Insufficient = Not able to say single or multiple

Size of the rent (measuring the size of the rent) 1- good; 2- sufficient and 3- insufficient.
Good = able to accurately measure the rent. .
Sufficient = Able to measure the rent but not with much confidence.
Insufficient = Not able to measure the rent

Sub classification (based on the antigrade flow) 1- good; 2- sufficient and 3- insufficient.
Good = able to subclassifying the CCF
Sufficient = Able to subclassify but not with much confidence.
Insufficient = Not able to

What is the first option of treatment? (transarterial cavernous sac coliing / coil + onyx, transvenous sac coiling, balloon embolization, trapping the artery, stent grafting, flow diverter)
Quality of choice of response 1- good; 2- sufficient and 3- insufficient.
Able to choose one option.
Able to choose one option but not with much confidence
Not able to choose one option
Which is the preferred embolic agent? (balloon, coil, stent or liquid agents) ;
Quality of choice of response 1- good; 2- sufficient and 3- insufficient.

Master Chart (Annexure 3)

Sl No	Key	Subclass 3D Consensus	L of R 3D Consensus	N of R 3D Consensus	Subclass 3D R1	Subclass 3D R2	Subclass 2D R1	Subclass 2D R2	L of R 3D R1	L of R 3D R2	L of R 2D R1	L of R 2D R2	N of R 3D R1	N of R 3D R2	N of R 2D R1	N of R 2D R2	L of R Q of D 3D R1	L of R Q of D 3D R2	L of R Q of D 2D R1	L of R Q of D 2D R2	N of R Q of D 3D R1	N of R Q of D 3D R2	N of R Q of D 2D R1	N of R Q of D 2D R2	S of R 3D R1	S of R 3D R2	S of R 2D R1	S of R 2D R2	Subclass Q of D 3D R1	Subclass Q of D 3D R2	Subclass Q of D 2D R1	Subclass Q of D 2D R2	FT 3D R1	FT 3D R2	FT 2D R1	FT 2D R2	FT Q of R 3D R1	FT Q of R 3D R2	FT Q of R 2D R1	FT Q of R 2D R2	PEA 3D R1	PEA 3D R2	PEA 2D R1	PEA 2D R2	PEA Q of R 3D R1	PEA Q of R 3D R2	PEA Q of R 2D R1	PEA Q of R 2D R2	Final proceedure	Actual Embolic Agent
1	N2	2	5	1	2	2	3	3	5	4	5	4	1	1	1	1	1	1	2	2	1	1	2	2	1	1	2	3	1	1	1	2	1	1	1	1	1	1	2	2	1	1	1	1	1	1	2	2	2	
2	LP3	1	1	1	1	1	2	2	1	1	1	2	2	1	1	1	1	1	2	3	1	1	2	2	1	1	2	3	1	1	3	2	1	1	1	1	1	1	1	2	2	2	1	1	1	2	3	1	3
3	SK4	1	2	1	2	1	1	1	2	2	3	3	2	1	1	1	1	1	2	2	1	1	2	2	1	1	3	3	1	1	1	2	1	1	1	1	1	1	2	1	1	1	1	2	1	1	2	3	2	
4	M5	1	1	1	2	3	1	2	1	1	2	3	1	1	1	3	1	1	2	3	1	1	2	3	1	1	2	3	1	1	1	2	1	1	1	1	1	1	2	1	1	1	1	1	2	3	2		
5	T6	1	5	1	1	1	1	1	5	5	3	5	1	1	1	1	1	1	2	3	1	1	2	2	1	1	2	3	1	1	1	2	1	1	1	1	1	1	2	1	1	2	1	2	1	1	2	1	1	2
6	RB7	3	5	1	2	3	3	3	5	4	5	2	1	1	1	1	1	1	2	1	1	1	2	2	1	1	2	3	1	1	1	2	1	1	1	1	1	1	2	2	1	1	1	1	2	2	1	1	1	
7	P9	1	1	1	1	1	1	1	1	1	1	1	1	1	1	1	2	2	2	2	1	2	2	2	1	1	2	2	1	2	1	2	1	2	1	2	2	1	2	1	2	2	1	1	2	2	2	1	1	
8	AR10	1	3	1	1	1	1	2	3	3	3	2	1	1	1	1	1	1	2	1	1	2	2	2	1	1	3	3	1	1	1	2	1	1	1	1	1	1	1	2	1	1	1	1	1	2	1	1	1	
9	B11	2	1	1	2	2	3	3	1	1	1	2	2	1	1	1	1	1	2	2	1	1	2	2	1	1	2	3	1	1	1	2	2	2	1	2	1	2	2	3			1				2		2	
10	N12	1	1	1	2	1	3	2	1	2	3	2	3	1	1	1	1	2	2	2	1	2	2	2	1	2	2	3	1	2	1	2	2	1	1	2	1	1	2	3		1	1			2	2		1	1
11	J13	3	5	1	3	2	3	3	5	5	5	4	2	1	1	1	1	1	2	2	1	1	2	2	1	1	2	3	1	1	1	2	2	2	1	1	2	2			1				2		2		
12	SK14	2	3	1	2	2	3	2	3	3	3	3	1	1	1	1	1	1	2	2	1	1	2	2	1	1	2	3	1	1	1	2	1	1	1	1	1	1	2	1	1	1	1	1	1	2	1	1	1	
13	GS15	1	1	1	1	1	3	3	1	1	1	2	1	1	1	3	1	1	2	2	1	1	2	3	1	1	3	3	1	1	1	2	1	1	1	2	1	2	2	2	1	1	1		1	2	2		2	
14	GA32	2	5	1	2	2	2	2	5	4	5	5	1	1	1	1	1	1	2	1	1	1	2	1	1	1	2	1	1	1	2	1	1	1	2	1	1	2	1	2	1	1	2	1	1	2	1	1	2	
15	SH35	2	3	1	2	2	1	2	3	3	3	3	1	1	1	1	1	1	2	2	1	1	2	3	1	1	2	3	1	1	1	2	1	1	1	1	1	1	2	3	1	1	1	1	1	2	3	1	1	
16	SK36	1	4	1	2	1	1	1	4	4	4	2	1	1	1	1	1	1	2	1	1	1	2	1	1	1	2	1	1	1	1	1	1	1	1	1	1	1	1	2	1	2	2	1	1	1	1	2	1	2
17	RJ37	2	1	1	2	2	3	3	1	1	3	2	1	1	1	1	1	1	2	3	1	2	2	3	1	2	2	3	1	1	1	2	2	2	1	1	1	1	2	2			1	2			2	3	2	
18	MM38	2	2	1	2	2	1	1	1	2	1	2	1	1	1	1	1	1	2	1	1	1	2	2	1	1	1	2	1	1	1	2	1	1	1	1	1	1	2	1	2	2	1	1	1	2	2	2	1	1
19	A39	1	1	1	1	1	3	2	1	5	1	1	1	1	1	3	1	1	2	2	1	1	2	3	1	1	2	3	1	1	1	2	1	1	1	1	1	1	2	1	1	2	1	2	1	1	2	3	1	1
20	SR40	1	1	1	1	1	1	1	1	1	1	2	1	1	1	1	1	1	2	2	1	1	2	2	1	1	3	3	1	1	1	2	1	1	1	1	1	1	2	1	1	1	1	2	1	1	2	2	1	1
21	PK41R	2	1	1	2	2	3	3	1	2	1	3	1	1	1	1	1	1	2	2	1	1	2	2	1	1	2	3	1	1	1	2	1	2	1	2	1	1	2	2	1			1		2		2		
22	PK41L	1	3	1	1	1	3	1	3	4	3	4	1	1	1	1	1	1	2	2	1	1	2	2	1	1	2	3	1	1	1	2	1	1	1	1	1	1	2	1	1	1	1	2	1	1	2	1	1	1
23	S42	1	4	1	1	1	1	1	5	4	4	4	1	1	1	1	1	1	2	1	1	1	2	1	1	1	2	1	1	1	1	1	1	1	1	1	1	1	2	1	1	2	1	1	1	1	2	2	1	2
24	JC46	2	4	1	1	3	3	3	4	4	5	4	1	1	1	1	1	1	2	1	1	1	2	2	1	1	2	3	1	1	1	2	1	2	1	2	1	1	2	2	2			1		1		2		
25	JP49	1	3	1	1	1	1	3	3	3	4	1	1	1	1	1	1	1	2	1	1	1	2	1	1	1	2	1	1	1	1	1	2	1	1	1	1	1	2	1	1	1	1	1	1	2	1	1	1	1
26	KT50	1	1	1	1	1	3	3	1	1	1	3	1	1	1	1	1	1	2	3	1	2	2	3	1	2	2	3	1	2	1	2	1	2	1	2	1	1	2	3	1			1		1		2		
27	RS51	3	4	1	2	3	3	3	5	4	5	4	1	1	1	1	1	1	2	2	1	1	2	2	1	1	2	3	1	1	1	2	1	2	1	2	1	1	2	2	1			2		1		2		
28	SS52	1	2	1	3	1	3	3	3	2	3	3	1	1	1	1	1	1	2	1	1	2	2	2	1	1	3	3	1	1	1	2	1	1	1	2	1	1	2	3	2	1	1		1	1	2		2	
29	VV54	2	3	1	2	2	2	2	3	3	3	3	1	1	1	1	1	1	2	1	1	1	2	1	1	1	3	1	1	1	1	1	1	1	1	2	1	2	1	1	1	1	1	2	1	1	2			
30	BA59	1	1	1	1	1	1	2	1	1	1	1	1	1	1	1	1	1	1	1	1	1	1	1	1	1	1	2	1	1	1	2	1	1	1	1	1	1	1	1	2	1	1	2	1	1	2	1	1	1
31	AT60	2	2	1	2	3	2	1	2	2	2	2	1	1	1	1	1	1	2	1	1	1	2	1	1	1	2	1	1	1	1	2	1	2	1	2	1	1	1	2	1		2		2		1		1	2
32	SK62	3	4	1	3	3	3	3	5	4	5	4	1	1	1	1	1	1	2	1	1	1	2	2	1	1	3	2	1	1	1	2	2	2	2	1	1	2	1									2		
33	SV63	1	2	1	2	1	2	2	1	2	1	3	1	1	1	1	1	1	2	3	1	1	3	3	1	1	3	3	1	1	1	2	1	1	1	1	1	2	1	1	1	1	1	1	1	2	3	2		
34	SK64	2	2	1	2	2	2	1	2	2	2	2	1	1	1	3	1	1	2	2	1	1	2	3	1	1	2	3	1	1	1	2	1	1	1	1	1	1	2	1	1	1	1	2	1	1	2	1	1	1
35	A65	1	2	1	1	1	1	1	3	2	3	3	1	1	1	1	1	2	2	3	1	2	3	3	1	1	3	3	1	1	1	2	1	1	1	1	1	1	2	3	2	1	2	1	1	1	2	3	1	2
36	FA67	1	2	1	1	1	2	2	2	2	3	3	1	1	1	2	1	1	2	2	1	1	2	3	1	1	2	3	1	1	1	2	1	1	1	1	1	1	2	2	2	2	2	2	1	1	2	2	1	2
37	KM68	2	2	1	2	2	3	2	3	3	3	3	1	1	1	1	1	1	2	3	1	1	3	3	1	1	3	3	1	1	1	2	2	2	1	1	2	1	3	3			2	1			2	3	2	
38	AB69	1	4	1	1	1	1	1	4	4	4	4	1	1	1	1	1	1	1	1	1	1	1	1	1	1	1	1	1	1	1	1	1	1	1	1	1	1	1	1	2	2	2	2	1	1	1	1	1	2
39	SP70	1	4	1	1	1	1	1	4	4	4	4	1	1	1	1	1	1	2	1	1	1	2	1	1	1	3	1	1	1	1	1	2	1	2	2	2	2	2	1	1	2	1	1	2	1	1	2		
40	Sa71	3	1	1	3	3	3	3	2	2	1	2	1	1	1	1	1	1	2	2	1	1	2	2	1	1	3	3	1	1	1	2	2	2	1	1	1	1	2	3			1	1			2	3	2	
41	TS72	2	1	1	2	1	3	2	1	1	3	2	1	1	1	1	1	1	2	1	1	1	2	2	1	1	3	3	1	1	1	2	1	1	1	1	1	1	2	3	1	1	1	1	1	2	2	3	1	1
42	BM73	1	3	1	2	1	2	2	3	3	2	2	1	1	1	1	1	1	3	2	1	1	3	2	1	1	3	2	1	1	1	2	2	1	1	1	1	1	2	2	1	1	1	1	2	2	1	1	1	
43	MM77	1	3	1	1	1	1	1	1	3	1	3	1	1	1	1	1	1	1	1	1	1	1	1	1	1	1	1	1	1	1	1	1	1	1	1	1	1	2	2	2	2	1	1	1	1	1	2		
44	TA81	2	1	1	2	2	2	2	1	1	3	3	1	1	1	1	1	1	2	2	1	1	3	2	1	1	2	3	1	1	1	2	1	1	1	1	1	1	2	2	1	1	1	2	1	2	2	2	1	1
45	SVV82	1	4	1	1	1	1	1	3	4	0	4	1	1	0	1	1	1	3	2	1	1	3	2	1	1	3	2	1	1	1	2	1	1	1	1	1	1	2	1	2	2	2	2	1	1	2	1	1	2

Plagiarism Checker X Originality Report

Comparison Of 3d Rotational Angiography With Digital Subtraction Angiography In Sub Classification And Treatment Planning Of Direct Carotid Cavernous Fistula

Similarity Found: 10%

Date: Friday, October 06, 2017
Statistics: 1669 words Plagiarized / 15984 Total words
Remarks: Low Plagiarism Detected - Your Document needs Optional Improvement.

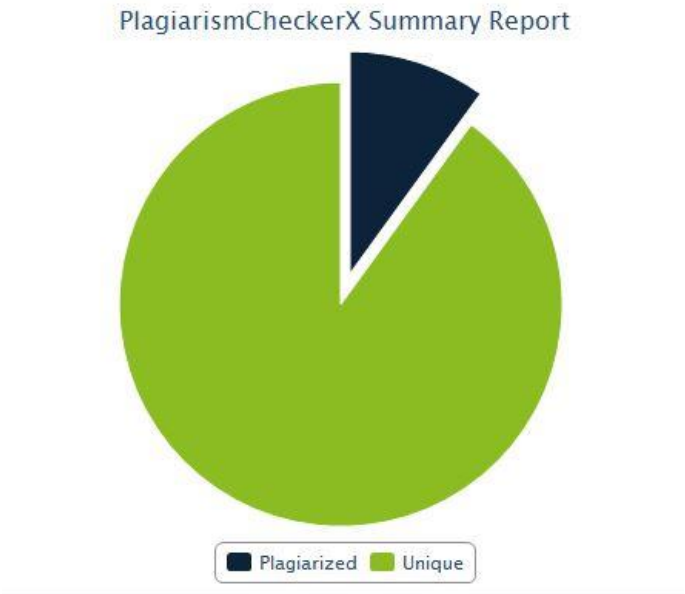

INTERNET SOURCES:

0% - https://www.researchgate.net/profile/Sah
0% - https://link.springer.com/chapter/10.100
0% - http://thejns.org/doi/10.3171/2012.2.FOC
0% - Empty
0% - https://www.wjgnet.com/1949-8470/full/v5
0% - https://link.springer.com/article/10.100
0% - http://www.clevelandclinicmeded.com/live
0% - https://issuu.com/libra64/docs/003987bra

0% - https://sites.google.com/site/dnbstudyma
0% - https://link.springer.com/content/pdf/10
0% - http://www.oired.vt.edu/sanremcrsp/wp-co
0% - https://academic.oup.com/europace/articl
0% - http://pubs.rsna.org/doi/full/10.1148/ra
0% - https://link.springer.com/article/10.100
0% - http://sam.gov/
0% - https://en.wikipedia.org/wiki/Infectious
0% - https://link.springer.com/chapter/10.100
0% - https://www.researchgate.net/publication
0% - https://link.springer.com/article/10.100
0% - https://www.aao.org/eyenet/article/diagn
0% - https://en.wikipedia.org/wiki/Stroke
0% - http://www.neurosurgery.theclinics.com/a
0% - http://www.neuroimaging.theclinics.com/a
0% - https://www.researchgate.net/publication
0% - http://www.sciencedirect.com/science/art
0% - https://radiologykey.com/carotid-caverno
0% - http://www.neurologyindia.com/article.as
0% - http://www.mdpi.com/2079-9721/4/2/19/xml
0% - https://academic.oup.com/qjmed/article/9
0% - https://issuu.com/duvalcountymedicalsoci
0% - http://www.journal-surgery.net/article/S
0% - http://www.medscape.com/medline/abstract
0% - http://thejns.org/doi/pdf/10.3171/2016.5
0% - https://link.springer.com/content/pdf/10
0% - http://www.jefferson.edu/content/dam/tju
0% - http://europepmc.org/articles/PMC3609701
0% - http://thejns.org/doi/10.3171/2016.5.JNS
0% - https://patents.google.com/patent/US5354
0% - https://issuu.com/duvalcountymedicalsoci
0% - http://www.thefoa.org/tech/ref/basic/ter
0% - https://www.everycrsreport.com/reports/R
0% - https://link.springer.com/article/10.100
0% - https://radiologykey.com/neuroradiology/
0% - https://www.wjgnet.com/1949-8470/full/v5
0% - http://www.sciencedirect.com/science/art
0% - http://www.neuroimaging.theclinics.com/a
0% - https://www.wjgnet.com/1949-8470/full/v5
0% - https://link.springer.com/chapter/10.100
0% - http://www.neurosurgery.theclinics.com/a
0% - https://rd.springer.com/content/pdf/10.1
0% - https://www.researchgate.net/publication
0% - https://www.healthline.com/health/head-i
0% - http://www.neuroimaging.theclinics.com/a
0% - https://www.researchgate.net/publication
0% - http://forensicpathologyonline.com/E-Boo
0% - https://link.springer.com/content/pdf/10
0% - http://www.ajnr.org/content/24/9/1789
0% - https://www.wjgnet.com/1949-8470/full/v5
0% - http://www.sciencedirect.com/science/art
0% - http://www.neurosurgery.theclinics.com/a
0% - http://europepmc.org/articles/PMC3380396
0% - http://stroke.ahajournals.org/content/st